Available online at www.sciencedirect.com
ScienceDirect
Journal of Theoretical Biology 251 (2008) 137–158
Journal of Theoretical Biology
www.elsevier.com/locate/yjtbi

Angiogenesis in bone fracture healing: A bioregulatory model

Liesbet Geris[a,*], Alf Gerisch[b], Jos Vander Sloten[a], Rüdiger Weiner[b], Hans Van Oosterwyck[a]

[a]Division of Biomechanics and Engineering Design, Katholieke Universiteit Leuven, Celestijnenlaan 300C (PB 2419), 3001 Leuven, Belgium
[b]Institut für Mathematik, Martin-Luther-Universität Halle-Wittenberg, 06099 Halle (Saale), Germany

Received 24 July 2007; received in revised form 7 November 2007; accepted 9 November 2007
Available online 19 November 2007

Abstract

The process of fracture healing involves the action and interaction of many cells, regulated by biochemical and mechanical signals. Vital to a successful healing process is the restoration of a good vascular network. In this paper, a continuous mathematical model is presented that describes the different fracture healing stages and their response to biochemical stimuli only (a bioregulatory model); mechanoregulatory effects are excluded here. The model consists of a system of nonlinear partial differential equations describing the spatiotemporal evolution of concentrations and densities of the cell types, extracellular matrix types and growth factors indispensable to the healing process. The model starts after the inflammation phase, when the fracture callus has already been formed. Cell migration is described using not only haptokinetic, but also chemotactic and haptotactic influences. Cell differentiation is controlled by the presence of growth factors and sufficient vascularisation. Matrix synthesis and growth factor production are controlled by the local cell and matrix densities and by the local growth factor concentrations. Numerical simulations of the system, using parameter values based on experimental data obtained from literature, are presented. The simulation results are corroborated by comparison with experimental data from a standardised rodent fracture model. The results of sensitivity analyses on the parameter values as well as on the boundary and initial conditions are discussed. Numerical simulations of compromised healing situations showed that the establishment of a vascular network in response to angiogenic growth factors is a key factor in the healing process. Furthermore, a correct description of cell migration is also shown to be essential to the prediction of realistic spatiotemporal tissue distribution patterns in the fracture callus. The mathematical framework presented in this paper can be an important tool in furthering the understanding of the mechanisms causing compromised healing and can be applied in the design of future fracture healing experiments.

Keywords: Bone regeneration; Fracture healing; Cell migration; Angiogenesis; Mathematical model

1. Introduction

1.1. Normal fracture healing

Bone is a tissue, unique in its scarless regenerative capacity. Under most circumstances bone truly regenerates itself, whereas soft tissue wound healing results in scar formation (Glowacki, 1998). The regeneration process of bone encompasses four overlapping phases: the inflammatory phase, the soft callus phase, the hard callus phase and the remodelling phase (Einhorn, 1995, 1998; Hadjiargyrou et al., 2002; Gerstenfeld et al., 2003a). Following bone injury, the cortical bone, periosteum and surrounding soft tissues are torn, rupturing numerous blood vessels. This is the start of the initial stage of fracture healing, the inflammation phase. As a consequence of the vascular trauma, the fracture site becomes hypoxic. Osteocytes at the fracture site become deprived of their nutrition and necrose, as do the damaged tissues in the fracture area. This necrotic process triggers an immediate inflammatory response, bringing inflammatory cells, leukocytes and macrophages to the region. These are followed by the invasion of fibroblasts, mesenchymal stem cells and endothelial cells (Taguchi et al., 2005). Growth factors and cytokines, important regulators of the healing process, are produced by the cells present in the regeneration area as well as released into this area from the surrounding tissues (damaged bone ends, muscles, periosteum, marrow)

*Corresponding author. Tel.: +32 16 328997; fax: +32 16 327994.
E-mail address: Liesbet.Geris@mech.kuleuven.be (L. Geris).
URL: http://www.mech.kuleuven.be/bmgo (L. Geris).

0022-5193/$ - see front matter © 2007 Elsevier Ltd. All rights reserved.
doi:10.1016/j.jtbi.2007.11.008

(Gerstenfeld et al., 2003a; Malizos and Papatheodorou, 2005). The initially formed granulation tissue is gradually being replaced by fibrous tissue, forming the soft callus.

In this soft callus, mesenchymal stem cells will start differentiating, guided by cues from their microenvironment, such as the presence of biological factors (Einhorn, 1998) and the perceived mechanical stimuli (Carter et al., 1998). Direct differentiation towards osteoblasts is observed near the cortex, away from the fracture site. These osteoblasts produce woven bone matrix, the hard callus, in a process called intramembranous ossification. Mesenchymal stem cells differentiate into chondrocytes (cartilage forming cells) in the, hypoxic, central fracture area where the soft callus will gradually take on the appearance of cartilage, mechanically stabilising the fracture zone. The chondrocytes mature towards hypertrophic chondrocytes, initiating biochemical preparations in the cartilage matrix to undergo calcification. This concludes the soft callus phase of healing.

In the next phase, the hard callus phase, osteoclasts, attracted by the growth factors secreted by the hypertrophic chondrocytes, degrade the mineralised cartilage matrix allowing blood vessels to invade the calcified cartilage which, in turn, bring along osteoblasts. These osteoblasts, receiving enough oxygen and subjected to the proper mechanical stimuli will produce a hard callus tissue consisting of mineralised woven bone matrix in a process called the endochondral ossification. When the fracture ends are connected by a bony callus, clinical union is reached. Already during the hard callus phase, the final remodelling phase begins with osteoclastic resorption of unnecessary or poorly placed parts of the callus by osteoclasts and the formation of lamellar bone. This remodelling takes place for a prolonged period of time, gradually reverting the blood supply to a normal state and restoring the bone to its original shape and strength.

1.2. Angiogenesis in fracture healing

Many local and systemic factors active during fracture healing have direct or indirect chondrogenic, osteogenic and/or angiogenic functions (Carano and Filvaroff, 2003). These factors include members of the fibroblast growth factor (FGF), transforming growth factor (TGF), bone morphogenetic protein (BMP) and vascular endothelial growth factor (VEGF) families. A detailed description of the biology of the growth factors involved in the above described processes can be found in Einhorn (1998), Barnes et al. (1999), and Dimitriou et al. (2005). The remainder of this section is focussed on the vascular growth factors.

Endogenous VEGF is a key player in bone repair, where its temporal and spatial expression pattern corresponds to the one observed during long bone development (Street et al., 2002). VEGF is essential for normal angiogenesis and appropriate callus architecture. More and more evidence is found to support the hypothesis that blood vessel invasion has a key role in tissue repair and VEGF production is the major coupling mechanism between angiogenesis and osteogenesis during fracture healing (Street et al., 2002). VEGF expression is induced in osteoblasts by various stimuli (overview in Carano and Filvaroff, 2003). In turn, VEGF regulates recruitment, survival and activity of osteoclasts, endothelial cells and osteoblasts (Street et al., 2002; Mayr-Wohlfart et al., 2002; Midy and Plouet, 1994; Deckers et al., 2000). Furthermore, VEGF has been observed to play a major role in cartilage maturation and resorption. Produced by hypertrophic chondrocytes, it initiates the endochondral ossification cascade by recruiting and/or differentiating osteoclastic cells that resorb cartilage and by attracting osteoblasts (Colnot et al., 2003; Maes et al., 2002).

Impaired angiogenesis plays an important role in the occurrence of non-unions (i.e. a failure to establish a bony bridging of the fracture gap) and delayed unions (i.e. a failure to establish a bony bridging of the fracture gap within a clinically reasonable period of time). Inhibition of the activity of VEGF or one of its homologues (e.g. placental growth factor, PlGF) disrupts the repair process and results in delayed union or non-union. Fracture healing experiments in $PlGF^{-/-}$ knock-out mice (Maes et al., 2006), show a reduced osteoblastic differentiation of mesenchymal progenitor cells and a persistent cartilaginous matrix without any sign of endochondral ossification. Angiogenesis, bone formation and callus mineralisation decrease when VEGF activity is inhibited in a mouse model of secondary fracture healing (Street et al., 2002). Severe vascular damage accompanying the skeletal injury during fracture, leading to an ischemic regeneration site, results in delayed union or non-union (Lu et al., 2007) with little cartilage or bone formation. In a distraction osteogenesis set-up, acute distraction (causing acute mechanical overload) disrupts the angiogenic process, preventing normal osteogenesis and resulting in fibrous non-union (Fang et al., 2005). In the same experimental set-up, fibrous non-union also occurs when proliferation of endothelial cells is blocked by an anti-angiogenic agent.

1.3. Mathematical modelling of fracture healing

Over the last decade, a number of mathematical models describing bone regeneration have been proposed. The first models were mechanoregulatory models, predicting bone formation based on local mechanical stimuli, in many cases making a distinction between the effects of the deviatoric and hydrostatic part of the stress or strain tensor. Several mechanoregulatory models were proposed (Prendergast et al., 1997; Carter et al., 1998; Claes et al., 1998) and were tested for various experimental situations, ranging from normal fracture healing (Lacroix and Prendergast, 2002), over distraction osteogenesis (Isaksson et al., 2006) to bone regeneration in an *in vivo* repeated sampling bone chamber (Geris et al., 2003, 2004, 2007). None of these models, however, takes the biological aspects of bone regeneration into account.

A few years after the appearance of these mechanoregulatory models, Bailón-Plaza and van der Meulen (2001) proposed a bioregulatory model of bone regeneration. This model does not take into account mechanical influences and describes fracture healing as a process regulated solely by osteogenic and chondrogenic growth factors (i.e. biological factors, hence the name bioregulatory model). The two-dimensional continuum model (system of partial differential equations, or PDE system), permits a detailed qualitative and quantitative comparison of the predicted spatiotemporal distribution of the different tissues with *in vivo* experimental observations. In Geris et al. (2006), this bioregulatory model was corroborated by applying the model to a semi-stabilised murine tibial fracture and comparing the simulation results with the experimental observations. In that study, also a first attempt was made to model situations of compromised fracture healing and to demonstrate the potential therapeutical value of bone regeneration models.

Some of the most recent models tried to combine both mechanical and biological factors. Bailón-Plaza and van der Meulen (2003) adapted their bioregulatory model and made a number of the model parameters dependent on the local mechanical environment. A fuzzy logic model was proposed by Shefelbine et al. (2005) to simulate fracture healing, based on local mechanical factors as described by Claes et al. (1998) and the local vascularity. To model the progress of angiogenesis in the fracture callus, a number of very basic, mechanoregulatory rules were applied. Finally, Gómez-Benito et al. (2005) presented a model describing fracture healing in terms of the evolution of the densities of different cell types in a growing callus. The regulatory component is only the local mechanical environment, neglecting again the influence of biological factors.

All of the aforementioned models lead to reasonable simulation results for normal fracture healing. However, there are still a number of limitations connected to these models when the simulation of compromised healing is envisaged.

(1) Most models only consider the influence of either the biology or the mechanics on the regeneration process.
(2) Cell migration, if present at all, is mostly treated as a simple diffusion process.
(3) None of the models (except the model of Shefelbine et al., 2005 but only in a very phenomenological way) includes the angiogenic process in the description of fracture healing.
(4) The models of Bailón-Plaza and van der Meulen (2001, 2003) do not make a distinction between the fibroblasts and chondrocytes, nor between the fibrous tissue component and the cartilaginous tissue component of the soft tissue callus.
(5) Endochondral ossification is described in a very phenomenological way by all models, as cartilage simply being replaced by bone without any reference to the underlying mechanisms.
(6) None of the aforementioned models (except the model of Gómez-Benito et al., 2005), modelled the growth and degradation of the fracture callus.

1.4. Objectives of this study

The main goals for this study are:

(1) The development of an enhanced bioregulatory model, incorporating a number of the bone regeneration key features such as intramembranous and endochondral ossification, angiogenesis and cell migration (numbers (2)–(5) on the list of shortcomings above).
(2) The investigation of possible causes of compromised fracture healing due to impaired angiogenesis.

In order to achieve these goals, the model presented here has started from the model proposed by Bailón-Plaza and van der Meulen (2001) and has extended it to include a description of the angiogenic process. Further modifications have been carried out to separate the descriptions of cartilage and fibrous tissue. Finally, the description of cell migration has been elaborated on to incorporate chemotaxis and haptotaxis as migratory mechanisms. The experimental system on which the model has been applied is the standardised externally fixated rodent fracture, developed by Harrison et al. (2003). The parameter values used for this model have been based on estimates obtained from experimental observations, if possible. Finally, a few of the aforementioned compromised situations due to impaired angiogenesis and other causes were simulated.

2. Materials and methods

2.1. Mathematical framework

The presented mathematical model is built on the model proposed by Bailón-Plaza and van der Meulen (2001). That model describes fracture healing as the spatiotemporal variation in density of seven variables: mesenchymal stem cells (c_m), chondrocytes (c_c), osteoblasts (c_b), a combined fibrous/cartilaginous extracellular matrix (m_c), bone extracellular matrix (m_b) and a generic osteogenic (g_b) and chondrogenic (g_c) growth factor. The model was extended with the following variables:

- the density of endothelial cells (c_v), a vascular matrix (m_v) and a generic angiogenic growth factor (g_v) for the description of angiogenesis;
- a variable representing the concentration of fibroblasts (c_f) and one describing the fibrous tissue density(m_f), thereby separating the variable m_c from the model of Bailón-Plaza and van der Meulen (2001) representing the combined fibrous/cartilaginous extracellular matrix

into two variables, the fibrous tissue (m_f) and the cartilage (m_c) density, respectively.

The mathematical model describing the interactions of these variables is a PDE model of taxis–diffusion–reaction type. The remainder of this section first gives an overview of the model equations and subsequently discusses the individual taxis and diffusion coefficient functions and the reaction terms. A schematic overview of the mathematical model is presented in Fig. 1.

According to the schematic representation in Fig. 1, the change in concentration or density of each of the models' variables is given by

$$\frac{\partial c_m}{\partial t} = \nabla[D_m \nabla c_m - C_{m_{CT}} c_m \nabla(g_b + g_v) - C_{m_{HT}} c_m \nabla m] + A_m c_m[1 - \alpha_m c_m] - F_1 c_m - F_2 c_m - F_4 c_m, \quad (1)$$

$$\frac{\partial c_f}{\partial t} = \nabla[D_f \nabla c_f - C_f c_f \nabla g_b] + A_f c_f[1 - \alpha_f c_f] + F_4 c_m - F_3 d_f c_f, \quad (2)$$

$$\frac{\partial c_c}{\partial t} = A_c c_c[1 - \alpha_c c_c] + F_2 c_m - F_3 c_c, \quad (3)$$

$$\frac{\partial c_b}{\partial t} = -\nabla[C_b c_b \nabla g_b] + A_b c_b[1 - \alpha_b c_b] + F_1 c_m + F_3 c_c - d_b c_b, \quad (4)$$

$$\frac{\partial c_v}{\partial t} = \nabla[D_v \nabla c_v - C_{v_{CT}} c_v \nabla g_v - C_{v_{HT}} c_v \nabla m_v] + A_v c_v[1 - \alpha_v c_v] - d_v c_v, \quad (5)$$

$$\frac{\partial m_f}{\partial t} = P_{fs}(1 - \kappa_f m_f) c_f - Q_f m_f m_c c_b, \quad (6)$$

$$\frac{\partial m_c}{\partial t} = P_{cs}(1 - \kappa_c m_c) c_c - Q_c m_c c_b, \quad (7)$$

$$\frac{\partial m_b}{\partial t} = P_{bs}(1 - \kappa_b m_b) c_b, \quad (8)$$

$$\frac{\partial m_v}{\partial t} = P_{vs}(1 - \kappa_v m_v) c_v, \quad (9)$$

$$\frac{\partial g_c}{\partial t} = \nabla[D_{gc} \nabla g_c] + E_{gc} c_c - d_{gc} g_c, \quad (10)$$

$$\frac{\partial g_b}{\partial t} = \nabla[D_{gb} \nabla g_b] + E_{gb} c_b - d_{gb} g_b, \quad (11)$$

$$\frac{\partial g_v}{\partial t} = \nabla[D_{gv} \nabla g_v] + E_{gvb} c_b + E_{gvc} c_c - g_v(d_{gv} + d_{gvc} c_v). \quad (12)$$

The Appendix describes the non-dimensionalisation of these equations, followed by a detailed discussion of the parameter values derived for this model.

The migration of *mesenchymal stem cells* is a combination of random and directed motion (Pountos and Giannoudis, 2005). The random motion was modelled as a haptokinetic process. The form of the haptokinetic coefficient was taken from Olsen et al. (1997), based on Dickinson and Tranquillo (1993). The latter model was corroborated by the experiments performed by Kuntz and Saltzman (1997) and Lutolf et al. (2003). Random motion is influenced by the total matrix density, defined as $m = m_f + m_c + m_b + m_v$, such that in the absence or

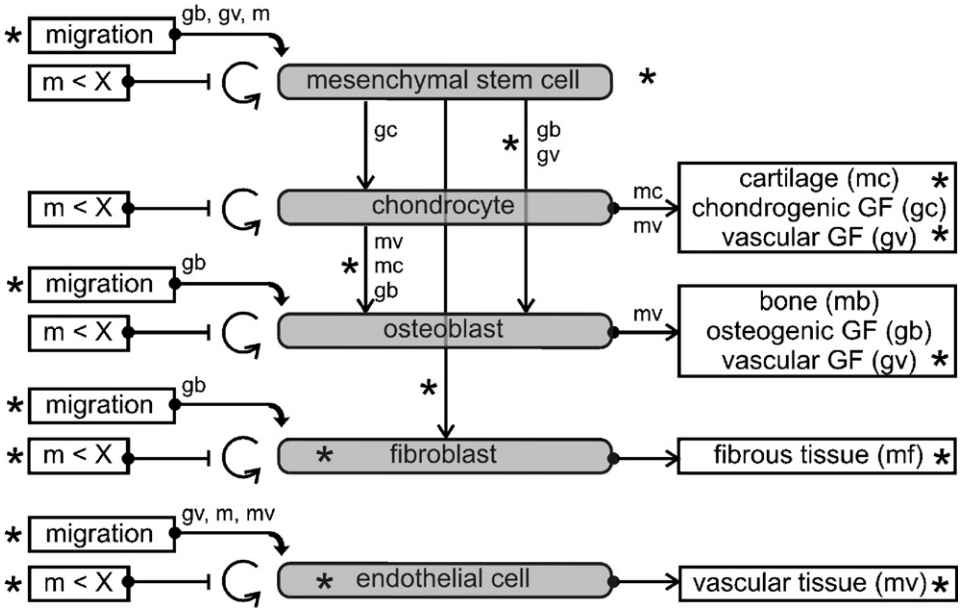

Fig. 1. Schematic overview of mathematical model. Legend: GF = growth factor, $m = m_f + m_c + m_b + m_v$ = total tissue density, X = maximum tissue density for proliferation, asterisks indicate extensions compared to Bailón-Plaza and van der Meulen (2001). The involvement of a variable in a regeneration subprocess is indicated by showing the name of that variable next to the arrow representing that particular process, e.g. the vascular matrix density interferes with cell migration, endochondral ossification and GF production.

abundance of extracellular matrix cells cease to move:

$$D_m = \frac{D_{hm} m}{K_{hm}^2 + m^2}. \tag{13}$$

Chemotaxis was modelled using a receptor-kinetic form, giving a maximum chemotactic response at a particular growth factor concentration, as was observed in experiments by Lind et al. (1996), Fiedler et al. (2004, 2005) and Metheny-Barlow et al. (2004). The chemotactic response of mesenchymal stem cells depends both on osteogenic and angiogenic growth factors:

$$C_{m_{CT}} = \frac{C_{kCTm}(g_b + g_v)}{K_{kCTm}^2 + (g_b + g_v)^2}. \tag{14}$$

The haptotactic coefficient was taken from Olsen et al. (1997), based on a kinetic analysis of a model mechanism for the cell-surface-receptor–extracellular-ligand binding dynamics (Sherratt, 1994):

$$C_{m_{HT}} = \frac{C_{kHTm}}{(K_{kHTm} + m)^2}. \tag{15}$$

The proliferation of stem cells, as well as the other four cell types, is modelled by a logistic growth function, whereby the proliferation rate depends on the surrounding matrix density (Olsen et al., 1997; Weinberg and Bell, 1985; Yoshizato et al., 1985):

$$A_i = \frac{A_{i0} m}{K_i^2 + m^2} \quad \text{for } i = m, f, c, b, v. \tag{16}$$

The differentiation of mesenchymal stem cells towards osteoblasts is mediated by the presence of osteogenic and angiogenic growth factors (Street et al., 2002; Mayer et al., 2005; Midy and Plouet, 1994). For high chemical concentrations, a saturation effect was modelled to take place (Bailón-Plaza and van der Meulen, 2001):

$$F_1 = \frac{Y_{11} g_b}{(H_{11} + g_b)} \cdot \frac{Y_{12} g_v}{(H_{12} + g_v)}. \tag{17}$$

A similar function, depending on the concentration of the chondrogenic growth factor, was used to model the differentiation towards chondrocytes:

$$F_2 = \frac{Y_2 g_c}{H_2 + g_c}. \tag{18}$$

The differentiation of mesenchymal stem cells into fibroblasts via the term $F_4 c_m$ is discussed below.

Fibroblasts invade the callus area from the surrounding tissues, but may also differentiate from mesenchymal stem cells. One of the regulators seems to be mechanical load whereby a high mechanical load stimulates the formation of fibroblasts (as e.g. hypothesised by Prendergast et al., 1997; Carter et al., 1998). However, this model does not explicitly treat the mechanical aspects of the regeneration process and therefore, as a first approximation, the differentiation rate of mesenchymal stem cells towards fibroblasts was taken to be a constant (F_4) (instead of a function of local mechanical stimuli). Very few studies report on the actions and functions of fibroblasts and fibrous tissue during fracture healing (Chai et al., 1999; Bland et al., 1999; Maheswari et al., 1999). Therefore, fibroblast migration and proliferation were described in a similar way as proposed by Olsen et al. (1995) in his model for wound healing. The random motion of fibroblasts was modelled by means of a constant diffusion rate (Olsen et al., 1995). For the directed migration of fibroblasts up the gradient of osteogenic growth factor concentrations, a receptor-kinetic form as given by Eq. (14), but only depending on g_b and not on g_v, was used. Upon the initiation of endochondral ossification, fibroblasts are removed from the callus (Zhang et al., 2001). This decay was modelled using replacement function F_3 (see Eq. (19)), to be discussed next, together with a proportionality factor d_f.

Endochondral replacement refers to the removal of mineralised cartilage and formation of bone. When *chondrocytes* exit their proliferative cycle, they will mature towards hypertrophic chondrocytes (Rossi et al., 2002). Exactly what causes the exit from the proliferative cycle and the subsequent differentiation towards hypertrophy is not well known. It involves amongst others a growth factor dependent triggering of proteins that induce growth arrest and proliferation slowdown (Enomoto-Iwamoto et al., 1998; Laplantine et al., 2002; Rossi et al., 2002). According to Einhorn (1998), the initiation of cartilage mineralisation is triggered by the abundance of cartilage. Combining these factors leads to the simplified representation of hypertrophic chondrocytes as chondrocytes that are no longer proliferating in the presence of a dense cartilage matrix (consistent with function (16) where the proliferation rate decreases for increasing matrix densities). Hypertrophic chondrocytes in the matrix start producing VEGF, attracting osteoclasts and endothelial cells into the mineralised matrix, increasing vascularity and triggering matrix metalloproteinases (MMPs) to degrade the cartilage matrix (Gerber et al., 1999; Deckers et al., 2002; Colnot et al., 2003). These cells are closely followed by osteoblasts laying down bone matrix. All these facts combined resulted in the following function for the endochondral replacement of chondrocytes:

$$F_3 = \frac{m_c^6}{(B_{ec}^6 + m_c^6)} \cdot \frac{m_v^6}{(B_v^6 + m_v^6)} \cdot \frac{Y_3 g_b}{(H_3 + g_b)}. \tag{19}$$

The first factor in this expression refers to the hypertrophy of the chondrocytes, the second factor to the invasion of blood vessels and the third factor to the attraction of osteoblasts, all of which are indispensable in the process of endochondral ossification. The actions of the osteoclasts are not explicitly included in the model, but their function is assumed in the above expression.

The functional form (19) was used to describe both the disappearance of chondrocytes from the cartilage and the introduction of new *osteoblasts* into the callus. These osteoblasts closely follow the endothelial cells upon the

invasion of the mineralised cartilage by blood vessels (Einhorn, 1998). The migration of osteoblasts is mainly due to chemotaxis, again using a functional form similar to form (14), but only depending on g_b and not on g_v. Upon production of bone matrix, osteoblasts gradually become entrapped by the matrix they are producing. When an osteoblast is completely surrounded by bone matrix, it will either mature and become an osteocyte or die (apoptosis). In both cases, this removes the osteoblast from the active matrix producing population and was modelled by a constant decay term.

Endothelial cells migrate in and towards the callus from the intact vasculature surrounding the fracture zone. This migration has a random movement component, modelled identical to the haptokinesis of mesenchymal stem cells (functional form (13)), and a directed movement component. Chemotactic migration up a gradient of vascular growth factor concentration was modelled again using the functional form (14), but this time only depending on g_v and not on g_b (Terranova et al., 1985), whereas haptotactic migration up a gradient of vascular tissue density was modelled using a constant haptotactic coefficient (Anderson and Chaplain, 1998). No distinction was made between tip cells, which have migratory capacities, and the quiescent endothelial cells, which do not. However, upon production of a collagenous vascular matrix, the endothelial cells become embedded and cease to migrate. This was modelled as the disappearance of endothelial cells with a constant decay rate. In that way, the variable c_v is representing the active cell pool, while the quiescent endothelial cells are enclosed in the vascular matrix, represented by variable m_v.

The spatiotemporal evolution of matrix densities was modelled according to Olsen et al. (1997) and Bailón-Plaza and van der Meulen (2001). *Extracellular matrix* production was assumed proportional to the cell density of the matrix producing cells, whereby the production rate decreases as the surrounding matrix density increases. The soft tissues (fibrous tissue and cartilage) have an additional degradation component, reflecting the removal of the respective tissue during the endochondral ossification process.

In most of the aforementioned processes, the local concentration of *growth factors* plays a key role. Growth factors are able to migrate inside the callus area, simulated here by a diffusion process with a constant diffusion coefficient (Anderson and Chaplain, 1998). Chondrogenic growth factors are produced by chondrocytes, up to a certain saturation concentration, after which the production rate levels off. For normal matrix densities, the production saturates and even decreases again for higher matrix densities. When chondrocytes become hypertrophic (simulated in this model by reaching a certain cartilage density, as previously elaborated), they cease to produce chondrogenic growth factors, and as they are removed during the endochondral ossification process, the production of chondrogenic growth factors drops to zero:

$$E_{gc} = \frac{G_{gc} g_c}{(H_{gc} + g_c)} \cdot \frac{m}{(K_{gc}^3 + m^3)}. \tag{20}$$

Removal of chondrogenic growth factors was modelled by a decay function (d_{gc}) representing denaturation and irreversible binding (Bailón-Plaza and van der Meulen, 2001). The production and decay of osteogenic growth factor were modelled in a similar way, except that the osteogenic growth factor production rate is not limited by matrix density:

$$E_{gb} = \frac{G_{gb} g_b}{H_{gb} + g_b}. \tag{21}$$

Angiogenic growth factors are produced both by osteoblasts and hypertrophic chondrocytes. The production rate is proportional to the present growth factor concentration (up to a saturation level) and also saturates for high vascular matrix densities, leading to the following function for the production rates by osteoblasts E_{gvb} and hypertrophic chondrocytes E_{gvc}:

$$E_{gvb} = \frac{G_{gvb} g_v}{(H_{gv} + g_v)} \cdot \frac{m_v}{(K_{gv}^3 + m_v^3)}, \tag{22}$$

$$E_{gvc} = \frac{G_{gvc} g_v}{(H_{gv} + g_v)} \cdot \frac{m_v}{(K_{gv}^3 + m_v^3)} \cdot \frac{m_c^6}{(B_{ec}^6 + m_c^6)}. \tag{23}$$

The final factor in the last equation refers again to the hypertrophy of the chondrocytes. The removal of vascular growth factor from the callus area, both through natural decay (d_{gv}) and through consumption by endothelial cells (d_{gvc}), was modelled by a simple uptake function (Anderson and Chaplain, 1998).

2.2. Simulation details

For the case of normal fracture healing, the standardised rodent fracture model developed by Harrison et al. (2003) was simulated. In this experimental set-up, a mid-diaphyseal femoral osteotomy was created in 12-week-old male Wistar rats and stabilised with a precision miniature external fixator in a unilateral, single plane configuration leaving a 0.5 mm osteotomy gap. Rats were sacrificed at several time points after fracture induction and the healing was assessed by (amongst others) histological analysis of the amounts of bone, cartilage and fibrous tissue in the callus area. A simplified axisymmetrical representation of the callus geometry was derived from a histological section of the callus at post fracture week 3 (Fig. 2). The expansion and regression of the callus geometry was not simulated in this study.

At the start of the simulation, the entire callus area was filled with a loose fibrous tissue matrix ($\tilde{m}_{f\_ini} = 0.1$). Resulting from the haemorrhage, vascular growth factor was present throughout the callus ($\tilde{g}_{f\_ini} = 10$). All other variables were assumed to be zero initially.

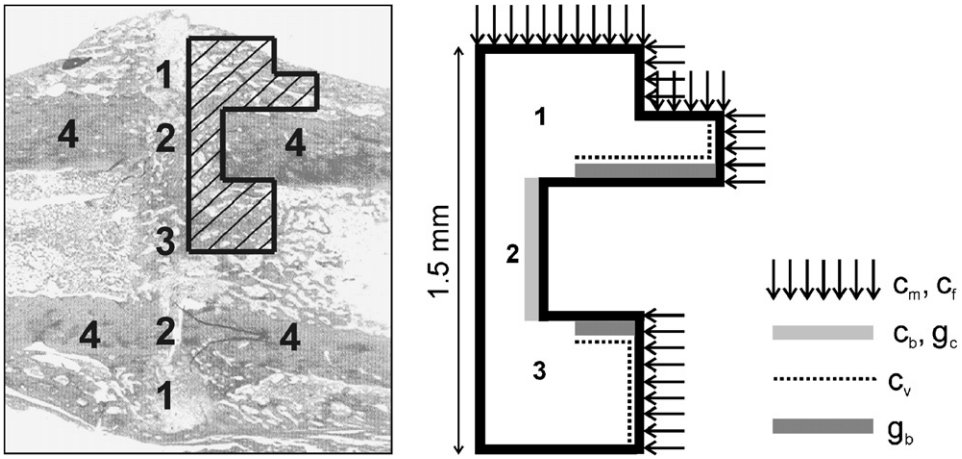

Fig. 2. Left: geometrical domain deduced from the real callus geometry at post fracture week 3. Right: Dirichlet boundary conditions, 1: periosteal callus; 2: intercortical callus; 3: endosteal callus; 4: cortical bone.

The mathematical model was closed by prescribing suitable boundary conditions. No-flux boundary conditions were applied for all components of the PDE system with diffusion or taxis terms, except for the situations, described below, where Dirichlet boundary conditions were prescribed for certain components on specific parts of the boundary and for a specified period of time. Mesenchymal stem cells and fibroblasts were released into the callus tissue at the beginning of the healing process from three possible sources: the periosteum, the surrounding soft tissues and the marrow space at the site of the damaged cortical tissue (Gerstenfeld et al., 2003a). The experimental set-up for normal healing simulated in this study did not compromise any of these sources (in contrast to one of the compromised healing set-ups discussed later on), therefore all sources were adopted here ($\tilde{c}_{m\_bc} = 0.02$ and $\tilde{c}_{f\_bc} = 0.02$ during first 3 days) (Fig. 2). Osteoblasts were modelled to originate from the degrading bone ends, but only in the very beginning of the healing process ($\tilde{c}_{b\_bc} = 1$ during the first 4 days). Contrarily, the intact vasculature in the cortical bone and marrow cavity were modelled as a source of endothelial cells throughout the entire regeneration process ($\tilde{c}_{v\_bc} = 10^{-4}$) (Gerstenfeld et al., 2003a). Chondrogenic and osteogenic growth factors were assumed to originate from, respectively, the fractured bone ends and the cortex away from the fracture site (Barnes et al., 1999; Dimitriou et al., 2005) ($\tilde{g}_{c\_bc} = \tilde{g}_{b\_bc} = 20$ during, respectively, 5 and 10 days).

2.3. Numerical implementation

The 12 variables $\vec{c}(t, \vec{x})$ in the model (1–12) are non-negative. This qualitative property of the solution must be inherited by its numerically computed approximation because, amongst others, erroneous negative values for the concentrations might render otherwise stable reaction terms unstable. Besides ensuring non-negativity, the algorithm employed for the numerical solution of the model must respect conservation of mass. The finite volumes technique was employed for its inherent mass conservation properties. The method of lines (MOL) was applied to separate the spatial and temporal discretisation (Hundsdorfer and Verwer, 2003). The axisymmetric structure of the problem was employed to properly reduce the model to an equivalent problem in two-dimensional space, leading subsequently to an efficient spatial discretisation (Gerisch and Geris, 2007).

The spatial domain Ω was covered with an equidistant computational grid. After convergence tests the grid size was fixed at 0.05 mm in both directions. On this grid, the diffusion and reaction terms in the system of Eqs. (1)–(12) were discretised using, respectively, the standard second order central difference approximation and pointwise evaluation, which were found to be sufficient in terms of accuracy and to ensure non-negativity of the solution of the resulting ordinary differential equation (ODE) system. Contrarily, the discretisation of the taxis terms in this system of equations required the application of upwinding techniques with nonlinear limiter functions (van Leer limiter) to guarantee accurate, non-negative solutions of the MOL-ODE system (Gerisch, 2001; Gerisch and Chaplain, 2005). The order of the spatial approximation is two in general. For the time integration of the resulting stiff MOL-ODE system the code ROWMAP (Weiner et al., 1997) was used. The method's built-in automatic step size control ensures the error caused in each time step (local error) to remain below a user-prescribed tolerance while keeping the computational cost as low as possible.

3. Results

This section describes the results of the simulations using the model described in the previous section. First, in Section 3.1, the simulation results for a normal fracture healing case are shown, followed by an overview of the results obtained in the sensitivity analyses in Section 3.2.

Finally, Section 3.3 summarises the results for the application of the current model to various compromised healing set-ups. A short description of the experimental models that these compromised healing simulations are based on will be provided in Section 4.

3.1. Normal healing

Using the parameter values as described in the Appendix, the model predicts full ossification of the callus at 4 weeks post fracture. Fig. 3 shows the spatiotemporal evolution of the fibrous tissue, cartilage, bone and vascular tissue extracellular matrix density. Mesenchymal stem cells, fibroblasts and growth factors invade the callus area from the surroundings. Near the cortex, away from the fracture site, mesenchymal stem cells differentiate directly towards osteoblasts under the influence of the osteogenic growth factor. Intramembranous ossification can be observed from post fracture day (PFD) 5 onward. In the remainder of the callus, mesenchymal stem cells differentiate into chondrocytes, guided by the presence of chondrogenic growth factors. The predominant tissue types present in the callus after 1 week are fibrous tissue and cartilage (Fig. 4). When the cartilage matrix reaches its maximum density (from PFD 14 onwards), chondrocytes start producing vascular growth factor. This attracts endothelial cells into the callus, causing cartilage degeneration, followed by a rise in the concentration of osteoblasts, producing bone matrix. Full vascularisation and ossification of the callus is reached 4 weeks after fracture induction.

3.2. Sensitivity analysis

Sensitivity analyses were carried out to assess the influence of the value of the parameters involved in the description of fibroblasts/fibrous tissue, cell migration and angiogenesis on the simulation outcome. The model shows robustness for small changes (parameter values between 10% and 1000% of the reference value given in the Appendix) in the parameters connected to fibroblasts and fibrous tissue. Large changes in those parameters (parameter values larger than 1000% or smaller than 10% of the original value) lead to a markedly increased number of fibroblasts or enhanced fibrous tissue density in the callus area and this subsequently influences the speed of the healing process and the location of the bony bridging of the fracture. The sensitivity analyses further indicated that the consumption of the vascular growth factor by the endothelial cells is essential for a normal fracture healing process. Consumption of the growth factor by the endothelial cells ensures the presence of a chemical gradient (of vascular growth factor) leading the endothelial cells further towards the source of the endothelial growth factor production (i.e. hypertrophic chondrocytes). As the concentration of chondrocytes producing vascular growth factor is lower in the endosteal zone, the healing process in this region is less affected by changes in the consumption rate (results not shown).

Additional sensitivity analyses were carried out to determine the importance of the initial conditions and the (location of the) boundary conditions on the simulation

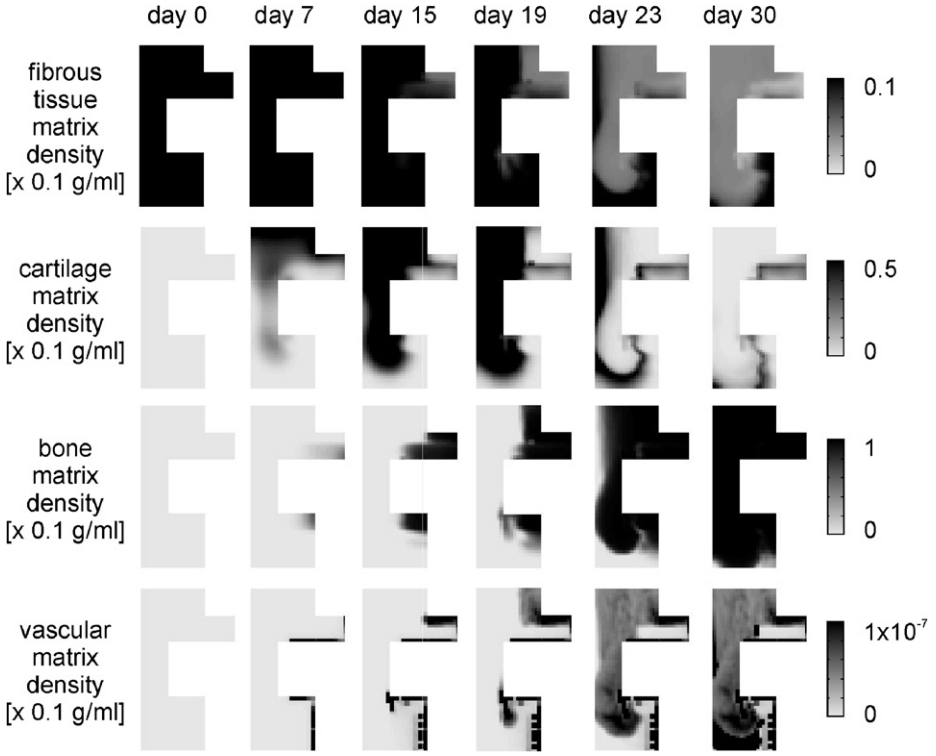

Fig. 3. Spatiotemporal evolution (days post fracture) of fibrous tissue, cartilage, bone and vascular matrix density.

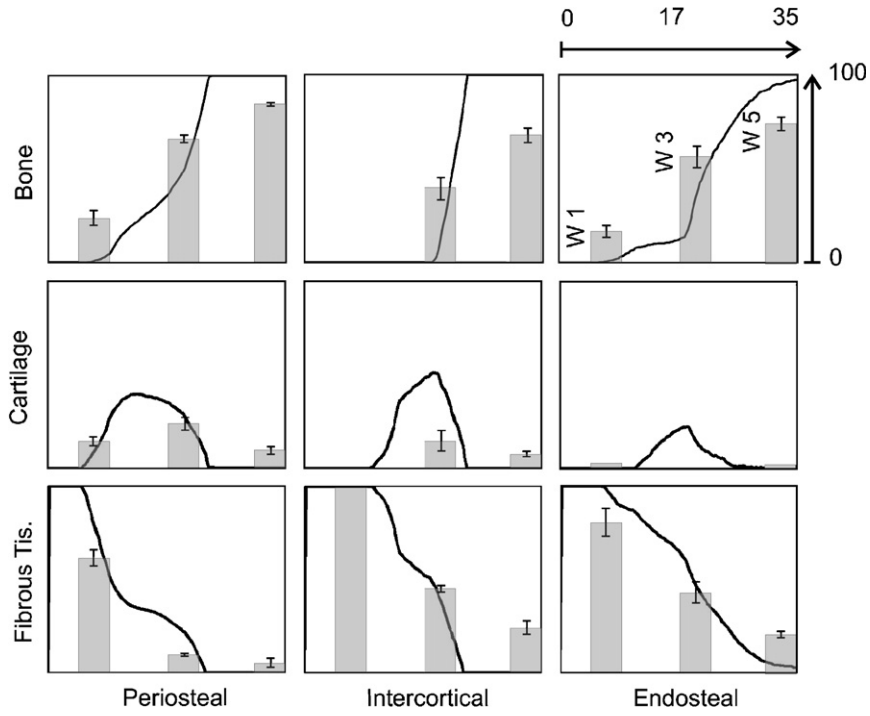

Fig. 4. Predicted (continuous line) and experimentally measured (bars, avg ± SE) tissue fractions (%) for the periosteal (left), intercortical (middle) and endosteal callus (right). The bars represent the histologically measured values at post fracture weeks 1, 3 and 5.

results. The model shows robustness for small changes (parameter values between 10% and 1000% of the reference value) in most of the values of initial and boundary conditions. Only the initial fibrous tissue matrix density has a more pronounced effect on the rate and the pattern of healing, as shown in Figs. 5 and 6. The initial non-homogeneous distribution of fibrous tissue matrix density influenced both the speed of the healing process and the location of the bony bridging, depending on the absolute value and the gradient of the matrix density. Furthermore, under normal healing conditions (i.e. for the simulation of a normal healing experiment), the origin of chondrogenic growth factors, mesenchymal stem cells and fibroblasts is not important. These cells and growth factors all migrate throughout the callus in a matter of days after fracture initiation. The location of the boundary conditions for osteoblasts, endothelial cells and osteogenic growth factors, however, is crucial to obtain a good spatial distribution of the various tissues inside the callus region. Adding a boundary condition for the osteogenic growth factors in the marrow cavity resulted in a substantial decrease in the amount of cartilage predicted in the endosteal callus, with a maximum endosteal cartilage fraction of 5% (Fig. 7). Additionally, a slowdown of the ossification process in the endosteal callus area was observed.

3.3. Compromised healing

Angiogenesis is crucial for the predicted normal fracture healing process as shown in Figs. 8 amd 9. A reduced production of vascular growth factor by hypertrophic chondrocytes (10% of reference value of $\tilde{G}_{gvc}$) will cause a very slow invasion of the cartilage matrix by the endothelial cells (Fig. 8a). Intramembranous ossification is unaffected by this reduced production. Successful healing through endochondral ossification takes place after 5 weeks, with bridging occurring simultaneously in the periosteal and endosteal callus zone. Reducing the production of vascular growth factor by the hypertrophic chondrocytes even further (1% of reference value of $\tilde{G}_{gvc}$) (Fig. 8b) prevents any endochondral ossification or the initiation thereof, constituting a non-union. Removing the initial condition for the vascular growth factor (i.e. initial concentration of vascular growth factor equal to 0: $\tilde{g}_{v\_ini} = 0$), while allowing normal vascular growth factor production by hypertrophic chondrocytes, also leads to a lack of healing response. A little intramembranous bone formation is observed near the presence of the intact vasculature (Fig. 8c), but there are no signs of endochondral ossification, nor the initiation thereof, in a period of 5 weeks after fracture.

4. Discussion

First, Section 4.1 discusses the results obtained by the application of the current model to a normal healing experimental set-up. The simulation results are compared with the experimental results and with the results of a previous mathematical model describing bone regeneration. Furthermore the added value of the extended description of cell migration is demonstrated. In Section 4.2,

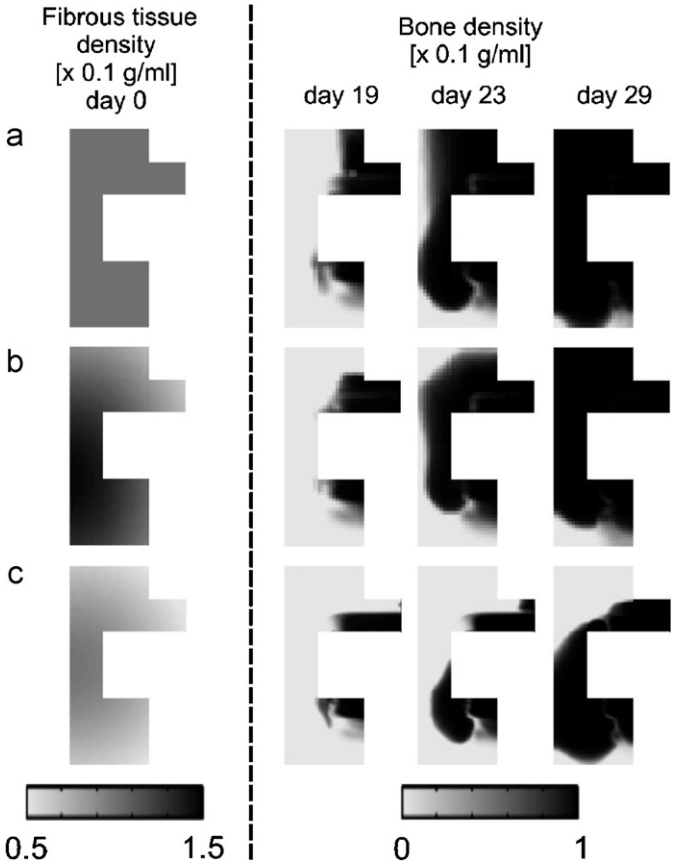

Fig. 5. Influence of the initial fibrous tissue matrix density on the progress of the healing process, shown for various initial fibrous tissue density distributions (left) and bone density (right) at various post fracture time points. (a) Reference situation (Fig. 3). (b) High, non-homogeneous initial fibrous tissue density. (c) Low, non-homogeneous initial fibrous tissue density.

the results of the sensitivity analyses both for the parameter values as for the initial and boundary conditions are addressed. In Section 4.3, the experimental set-ups of compromised healing situations are described and the outcome of the application of the current model to these cases is considered. The added value of using mathematical models in the investigation of compromised healing situations is discussed. Section 4.4 examines the limitations and potential extensions of the current model. Finally, Section 4.5 recapitulates the main goals and the most significant results of this study.

4.1. Normal healing

The presented model is able to capture essential features of the fracture healing process and demonstrates that angiogenesis and directed cell motility are key factors in the establishment of a successfully healed fracture. Fracture healing is described using a continuum system of equations, representing the spatiotemporal evolution of concentrations or densities of several cell types, extracellular matrix types and growth factors (Fig. 1). Parameter values were derived from literature if available and the model was applied to a highly quantified (in terms of tissue distribution) experimental set-up.

In the experiments reported by Harrison et al. (2003), the distribution of fibrous tissue, bone and cartilage for different zones of the callus were determined histologically at PFDs 7, 21 and 35. These values are represented by the bars in Fig. 4. The fibrous tissue density decreases, as the bone matrix density increases towards the end of the healing period. Meanwhile, the cartilage matrix density increases and subsequently decreases again. The ossification

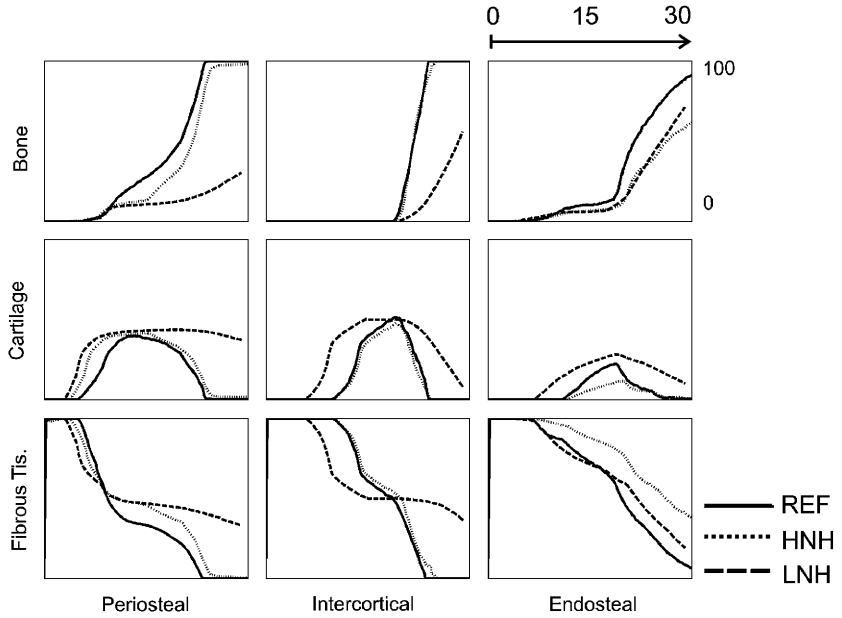

Fig. 6. Predicted tissue fractions (%) for the periosteal (left), intercortical (middle) and endosteal callus (right). The dashed and dotted lines represent various initial fibrous tissue density distributions. REF: reference situation (Fig. 4); HNH: high, non-homogeneous initial fibrous tissue density; LNH: low, non-homogeneous initial fibrous tissue density.

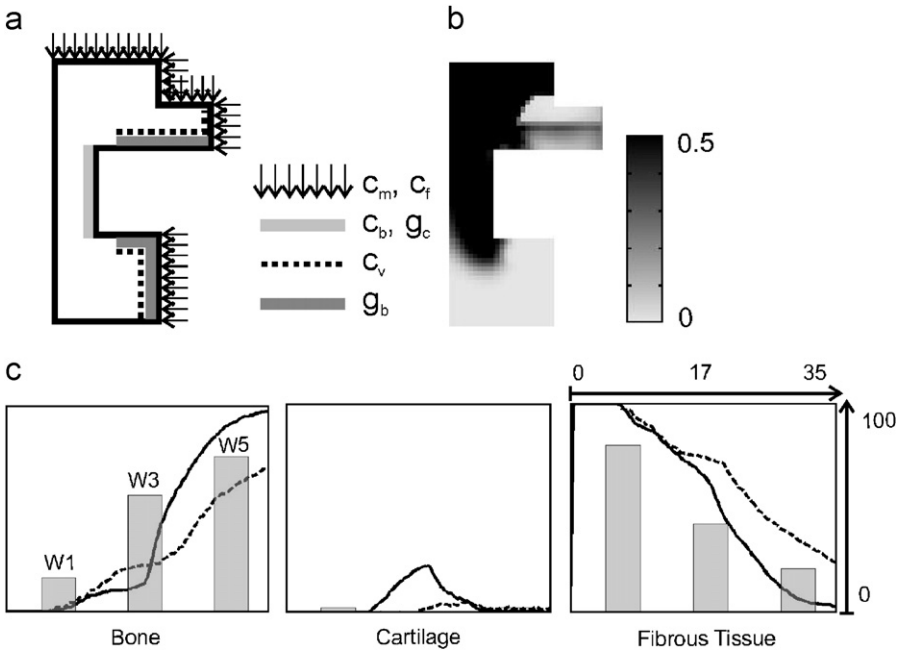

Fig. 7. Influence of additional boundary condition for osteogenic growth factor in the marrow cavity. (a) Boundary conditions. (b) Cartilage density (×0.1 g/ml) at 23 days after fracture, i.e. when the cartilage fraction in the callus reaches its maximal value. (c) Temporal evolution (days post fracture) of tissue fractions (%) in the endosteal callus for simulations with the boundary conditions shown in Fig. 2 (continuous line) and with additional boundary condition for the osteogenic growth factor g_b in the marrow cavity (dashed line). The bars represent the histologically measured values at post fracture weeks 1, 3, and 5.

process enrolls most rapidly in the periosteal callus and the healing process in the intercortical zone starts up last. Comparison of the simulation results with these experimental results, showed a good agreement between the theoretically predicted and experimentally observed changes in the distribution of different tissues in the callus (Figs. 3 and 4). Similar to the experimental observations, the transitions between the different tissue types were predicted to initiate first in the periosteal callus, followed by the endosteal callus and the intercortical callus. As to the latter zone, the transitions occurred very rapidly. Compared to the results obtained with the model of Bailón-Plaza and van der Meulen (2001) (as reported for a comparable rodent experimental setting in Geris et al., 2006), more realistic healing patterns were predicted by the current model, due to the influence of angiogenesis and directed cell migration. The current model predicted ossification fronts moving parallel to the fracture line (perpendicular to the cortex) towards the center of the fracture (Fig. 10b), as is experimentally observed in most rodent models (Harrison et al., 2003; Maes, 2004), whereas previously, the ossification fronts were predicted to move perpendicular to the fracture line from the external callus towards the central marrow cavity (Geris et al., 2006). Notably, depending on the animal model under investigation, external bridging followed by creeping substitution can take place. However, the isolated external bridging as predicted in (Geris et al., 2006), where a thin layer of bone is formed at the most external side of the callus, is not physiological. Furthermore, contrarily to the results reported using the model of Bailón-Plaza and van der Meulen (2001), a quantitative comparison with the experimental observations of all the experimentally measured tissue fractions in the callus (bone, cartilage and fibrous tissue) was possible, due to the addition of fibroblasts and fibrous tissue as separate variables in the current model (Fig. 10a). Further quantitative comparisons between the experimentally observed and numerically simulated regeneration process (e.g. cell and matrixdensities, growth factor concentrations) are hampered by the lack of available quantitative experimental data in the literature.

As stated above, the addition of angiogenesis and directed motion of cells to the model of Bailón-Plaza and van der Meulen (2001) resulted in more realistic healing patterns. Directed motion of endothelial cells is essential to derive the correct pattern of endothelial cell distribution throughout the callus. As observed in Fig. 11, in the absence of directed motion, endothelial cells spread throughout the entire callus rather than aligning at the ossification front (i.e. the interface between the mineralised cartilage and the newly formed bone) as experimentally observed (Maes, 2004). Although the time scale corresponds to that of the standardised fracture set-up (Fig. 12), the spatial evolution of the tissue fractions (e.g. location of callus bridging) and the endothelial cells (e.g. alignment at ossification front) in the callus does not (Fig. 11). Chemotaxis alone causes a too fast endochondral ossification in response to the vascular growth factors, produced

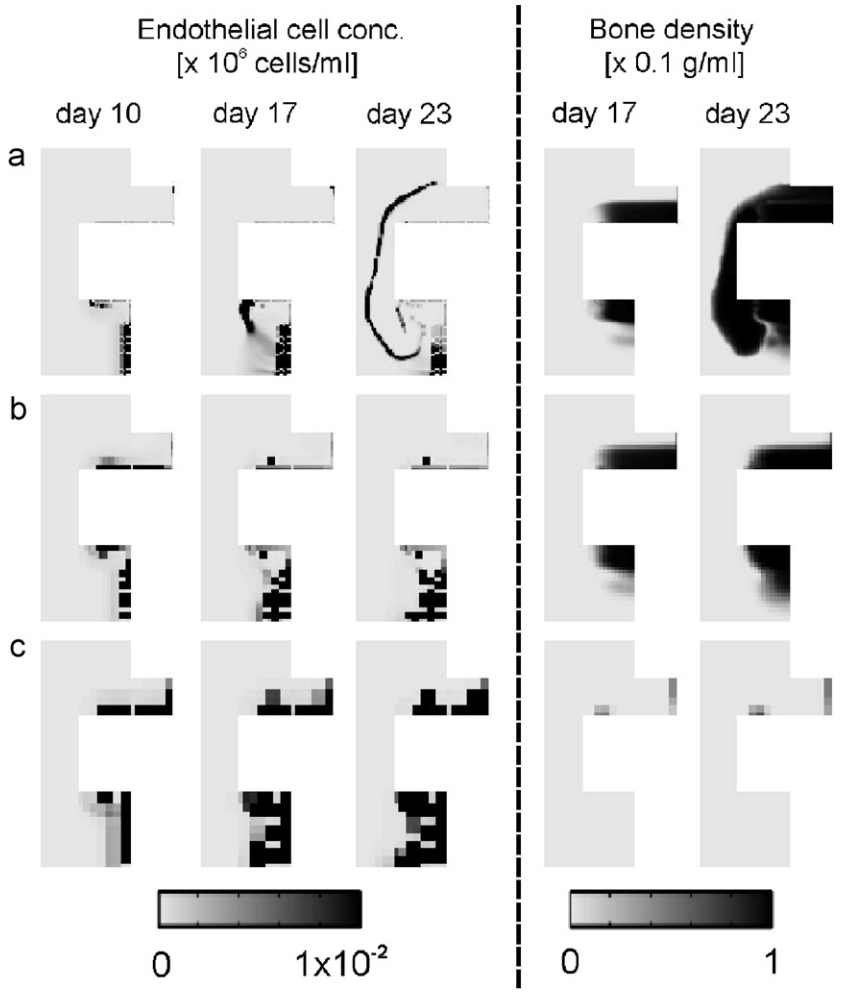

Fig. 8. Influence of the angiogenic process on fracture healing, shown by predicted endothelial cell concentration (left) and bone density (right) at various post fracture time points. (a) Reduced production (10% of reference value) of vascular growth factor by hypertrophic chondrocytes. (b) Further reduced production (1% of reference value) of vascular growth factor by hypertrophic chondrocytes. (c) Absence of vascular growth factor in callus at day 0.

by the chondrocytes, with a wide spread ossification front moving from the periosteal callus towards the endosteal callus. Only when haptotaxis is added, the correct alignment of endothelial cells in the zone between the degrading cartilage and the newly formed bone is obtained.

A discrepancy between the experimental observations and the model's predictions is the time frame. Whereas it takes 5 weeks in the experiments to establish successful healing, the model predicts a fully ossified callus after 4 weeks already. This, however, is an improvement compared to the model of Bailón-Plaza and van der Meulen (2001) which predicts full callus ossification in less than 3 weeks (comparison shown for the periosteal callus in Fig. 10a). There are several explanations for the observed discrepancy in the absolute timing of the healing events. One reason could be that the model does not capture the maturation of the cell and the time that elapses between the differentiation of mesenchymal stem cell towards osteoblast and the production of extracellular matrix by the matured osteoblast (Bruder and Scaduto, 2005). Another reason could be the fact that the parameter values have been derived based on both *in vivo* and *in vitro* experiments on different animal models and cell lines reported in the literature, or have been estimated when no information was available.

4.2. Sensitivity analysis

Sensitivity analyses indicated robustness of the model's predictions for small changes (parameter values smaller than 1000% or larger than 10% of the original value) in the parameter values related to the description of fibroblasts and fibrous tissue formation. Larger changes (parameter values larger than 1000% or smaller than 10% of the original value) lead to substantial increases in the fibrous tissue density and influence the speed of the healing process and the location of the bony bridging. Rapid formation of soft tissue matrix inhibits endothelial cell proliferation and migration into the callus, resulting in delayed ossification at that location. This numerically observed inhibition of

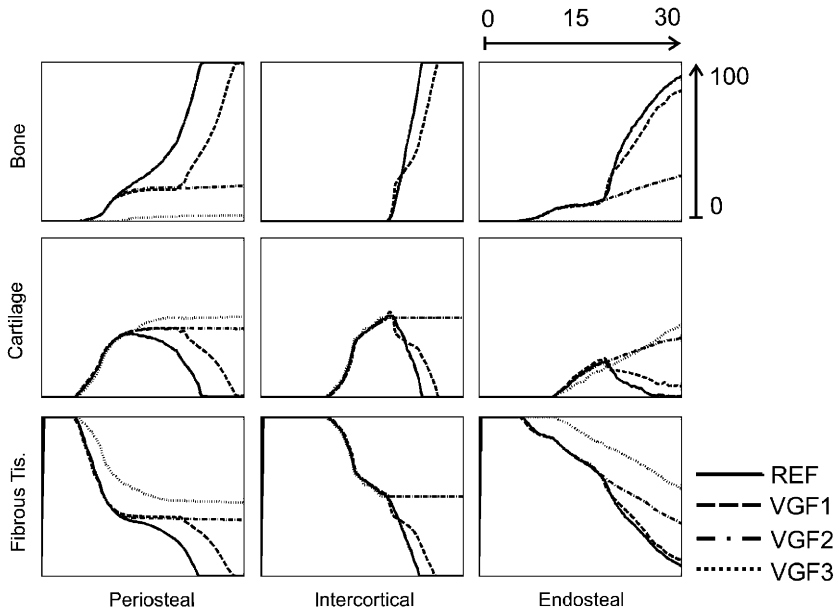

Fig. 9. Influence of the angiogenic process on tissue fractions (%) during fracture healing. Predicted tissue fractions for the periosteal (left), intercortical (middle) and endosteal callus (right). The dashed and dotted lines represent various compromised healing situations. REF: reference situation (Fig. 4); VG1: reduced production (10% of reference value) of vascular growth factor by hypertrophic chondrocytes; VG2: further reduced production (1% of reference value) of vascular growth factor by hypertrophic chondrocytes (bone fraction in the intercortical callus: 0%; cartilage and fibrous tissue fractions in the intercortical callus: 50%); VG3: absence of vascular growth factor in callus at day 0 (bone fraction in the intercortical and endosteal callus: 0%; cartilage and fibrous tissue fractions in the intercortical callus: 50%).

endothelial cell migration due to increased soft tissue matrix density is not corroborated by experimental observations. Migration of tumour cells, like endothelial cells, has been shown to depend both on chemical (e.g. matrix ligand and cell integrin receptor levels) and mechanical (e.g. stiffness of the substrate) cues from the environment (Zaman et al., 2006). Moreover, much like endothelial cells, tumour cell migration has been shown to on the proteolytic activity from broad-spectrum matrix MMPs (Zaman et al., 2006) to create a path through the existing matrix. Alternative functional forms for endothelial cells random motion and/or the incorporation of MMPs as an additional variable to the model, could further enhance the model's description of endothelial cell migration in soft tissues.

As chemotaxis is an essential part of the endothelial cells' migratory mechanism, the presence of a chemical gradient is needed for the good progression of fracture healing. Consumption of the vascular growth factor by endothelial cells ensures the maintenance of this gradient, guiding the endothelial cells towards the source of the vascular growth factor production (i.e. the hypertrophic chondrocytes). A decrease in the consumption rate of vascular growth factor by endothelial cells (10% of reference value of $\tilde{d}_{gvc}$) reduces the concentration gradient of vascular growth factors at the location of the endothelial cells, leading to a loss of the directional cue that guides them. Endothelial cell migration is disturbed (Nagy and Senger, 2006), leading to a disturbance in the angiogenic and hence endochondral ossification process. As the concentration of chondrocytes producing vascular growth factor is lower in the endosteal callus, endothelial cell migration in this region is less disturbed. Endochondral ossification starts up in the endosteal callus followed by bony bridging in that region.

Additional sensitivity analyses demonstrated robustness to the values of initial and boundary conditions. Only the initial fibrous tissue matrix density influences both the rate and the pattern of healing, due to its impact on the migration and proliferation of cells as explained above. The location of the boundary conditions for osteoblasts, endothelial cells and osteogenic growth factors was found to have a significant influence on the spatial distribution of the various tissues inside the callus region. For example, in the model intramembranous ossification was observed immediately next to the boundaries where osteogenic growth factors are released. Experimental observations have shown that condensation and osteoblastic differentiation of mesenchymal stem cells inside the marrow, reactivation of the osteoblasts lining the cortical bone surface and subsequent intramembranous ossification is also only taking place near the cortex away from the fracture site (Barnes et al., 1999). As processes in the marrow and cortex are not included in the mathematical model, these events need to be captured by the boundary conditions. Finally, in the experiments, hardly any cartilage was observed in the endosteal zone. Although the model also predicted the smallest amount of cartilage in this zone, it was still an overestimation with respect to the experiment. Most of the mesenchymal stem cells present in the endosteal zone originate from the bone marrow. Bone

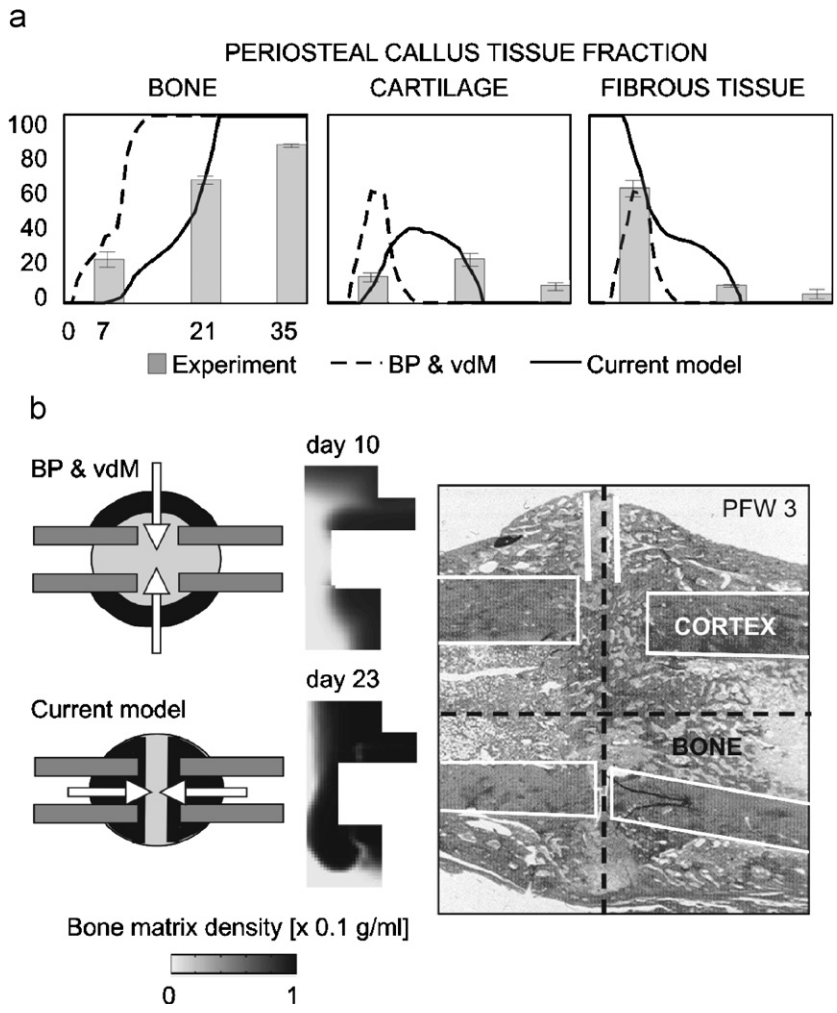

Fig. 10. Qualitative and quantitative improvements of the current model compared to the previously described bioregulatory model (Bailón-Plaza and van der Meulen, 2001). (a) Experimentally measured (bars, avg ± SE) and predicted tissue fractions (%) for the periosteal callus. Full line: current model; dashed line: model of (Bailón-Plaza and van der Meulen, 2001. (b) Qualitative comparison between experimentally observed (right) and predicted ossification fronts. The left figures are schematic representations of the direction of movement of the ossification fronts.

marrow derived cells have been shown to differentiate towards osteoblasts during fracture healing (Taguchi et al., 2005). This preference of the precursor cells was not captured by the model. A possible way to achieve this in the model would be to add a boundary condition for the osteogenic growth factors in the marrow cavity. When doing so, a substantial decrease in the amount of cartilage was encountered in the endosteal callus, with a maximum endosteal cartilage fraction of 5% (Fig. 7). Additionally, this caused a slowdown of the ossification process in the endosteal callus area. Another possibility to capture this preference in a more mechanistic way would be to introduce discrete differentiation stages for the osteoblasts, e.g. mesenchymal stem cell, osteoprogenitor, pre-osteoblast and osteoblast. The precursor cells originating from the marrow could than be modelled as osteoprogenitors or pre-osteoblasts rather than mesenchymal stem cells, indicating their osteogenic preference. This model extension will be further discussed below.

4.3. Compromised healing

The sensitivity of the model's predictions to the values of the parameters, involved in the initial presence and the production of the angiogenic growth factor, mimics the biological sensitivity of the healing process to these parameters. To illustrate this, different compromised conditions due to impaired angiogenesis as reported in literature, were simulated with the model. A first experiment that was simulated, was the one reported by Street et al. (2002), who investigated the effect of VEGF on (amongst others) secondary fracture healing in a rodent model. Mice were injected with a soluble VEGF receptor during the course of fracture repair. This led to a dramatic decrease in callus vascularity and new bone formation. As the binding of the vascular growth factor cannot be simulated with this model, the production of vascular growth factor by hypertrophic chondrocytes during fracture healing was reduced instead. A reduced production of

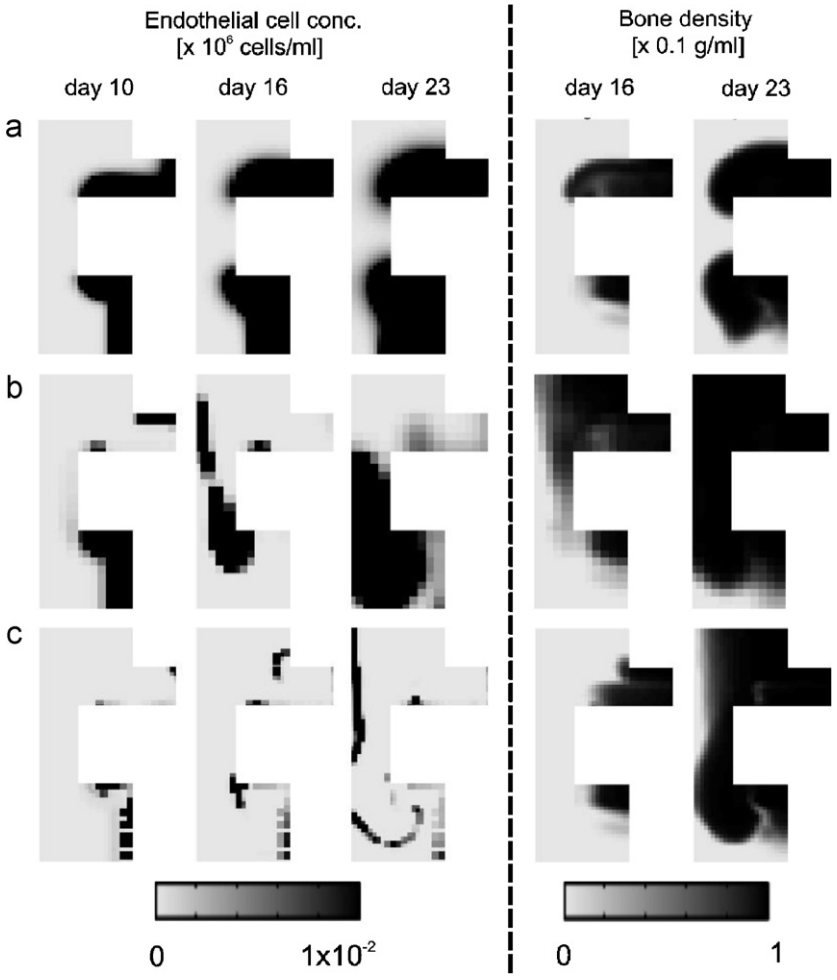

Fig. 11. Influence of migration of endothelial cells on fracture healing, shown by predicted endothelial cell concentration (left) and bone density (right) at various post fracture time points. (a) Only haptokinesis. (b) Haptokinesis and chemotaxis. (c) Haptokinesis, chemotaxis and haptotaxis.

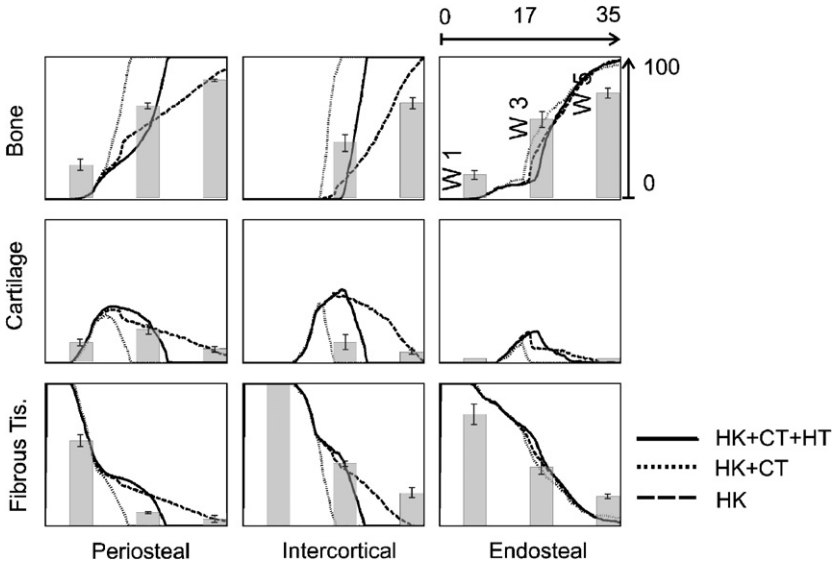

Fig. 12. Influence of migration of endothelial cells on tissue fractions (%). Predicted (lines) and experimentally measured (bars, avg ± SE) tissue fractions for the periosteal (left), intercortical (middle) and endosteal callus (right). The bars represent the histologically measured values at post fracture weeks 1, 3 and 5. The dashed and dotted lines represent situations with different descriptions of endothelial cell migration. HK: haptokinesis; CT: chemotaxis; HT: haptotaxis.

vascular growth factor caused a delayed healing response with a slow penetration of endothelial cells into the cartilage (Fig. 8). Further reduction of the vascular growth factor production rate prevented all endochondral ossification from taking place. A second experiment that was simulated was taken from Maes et al. (2006). In that experiment, a semi-stabilised tibial fracture was created in both wild-type and $PlGF^{-/-}$ mice (PlGF is a VEGF homologue). This resulted in a significant decrease in the amount of other vascular growth factors (e.g. VEGF) available at the beginning of the healing process. Furthermore, a persistent cartilaginous matrix and the absence of endochondral ossification were observed. This experiment was approximated in the simulations by taking the initial concentration of the vascular growth factor in the callus area equal to zero. This resulted, similar to the experimental observations, in a persistent cartilaginous matrix, with only a small amount of intramembranous bone, formed close to the cortex (Fig. 8). This model is the first in its kind capable of simulating compromised healing situations related to (impaired) angiogenesis. Ongoing work is looking into potential treatment strategies for these compromised healing situations.

This section clearly indicates the advantages of the current mathematical model over previous models in modelling compromised healing situations. In order to investigate the vast body of pathologies related to problems in the blood supply to the regeneration zone, the explicit modelling of the angiogenic process is essential.

4.4. Limitations of the model

For a number of the functional forms derived in the course of this study, such as the differentiation from mesenchymal stem cells towards osteoblasts (functional form (17)) and the removal of fibroblasts from the callus (functional form (19)), alternative formulations are possible. The currently implemented osteoblastic differentiation from mesenchymal stem cells requires the presence of both osteogenic and vascular growth factors. *In vivo*, vascular invasion is a prerequisite for endochondral bone formation and fracture healing (Bolander, 1992). Angiogenesis related factors may therefore affect osteoblast function or differentiation and vice versa (Guenther et al., 1986; Sato and Rifkin, 1988; Villenueva and Nimni, 1997; Kasperk et al., 1997; Deckers et al., 2000). However, *in vitro* experiments have shown osteoblastic differentiation solely influenced by osteogenic growth factors (Thies et al., 1992; Ahrens et al., 1993; Rickard et al., 1994). Altering the expression of the functional form to also allow for osteoblast differentiation solely under the influence of osteogenic growth factors did not significantly alter the predictions (neither qualitatively nor quantitatively). In the current model, fibroblasts undergo apoptosis when endochondral ossification takes place. However, also during intramembranous ossification, fibroblasts will either trans-differentiate towards osteoblasts or go into apoptosis (Lin et al., 1994; Hee et al., 2006). Introducing these aspects into the equations for both fibroblasts and fibrous tissue did not change the simulation outcome.

Alternative functional forms for various other processes described in this model will be addressed in future studies. As indicated above in Section 4.2, different functional forms for the random motion of endothelial cells need to be investigated in order to be able to capture the experimentally observed behaviour of endothelial cells in both soft and hard tissue environments.

As briefly mentioned in Section 2, one of the main limitations of this model is that it does not take into account the influence of mechanical loading on the regeneration process. Several cellular processes are known to depend on the experienced mechanical stimuli. Cell migration (Michaeli et al., 1994), cell proliferation (Kaspar et al., 2000), cell differentiation (Jagodzinski et al., 2004; Li et al., 2004; Kreke et al., 2005; Knippenberg et al., 2005), matrix synthesis (Bancroft et al., 2002) and growth factor production (Sakai et al., 1998; Pufe et al., 2005) have been shown to be influenced by mechanical loading (for reviews, see e.g. Darling and Athanasiou, 2003; Ehrlich and Lanyon, 2002). Furthermore, recent data suggests that mechanical loading interferes with angiogenesis, rendering this interaction one of the key regulators for successful bone formation during distraction osteogenesis and fracture healing (Amir et al., 2006; Fang et al., 2005; Lienau et al., 2005). Too high mechanical loads inhibit the formation of a vascular network, thereby inhibiting bone formation to occur. Furthermore, too high mechanical loading favours the differentiation of mesenchymal stem cells towards fibroblasts and severely hampers the formation of bone ECM. As mechanical loading may play a less important role in the smaller animal models such as the ones used in this study, the omission of mechanics may probably have a smaller impact on the simulation results than may be the case for the application of this mathematical model to larger animal models. However, the absence of mechanical loading in this model prevents it from being applied to investigate a whole range of compromised healing situations that involve over- or underloading of the callus area. The incorporation of the mechanical aspect of fracture healing into the model is the next obvious extension of the model.

When constructing the geometric model (Fig. 2), the dorsoventral and mediolateral asymmetry of the femur was not taken into account, as a generic model of a fracture callus is sufficiently accurate for the purpose of this study. Differences in the healing response for the different anatomical locations could be obtained by applying slightly different boundary conditions related to those specific locations. Furthermore, the boundary of the external callus was not accurately modelled since in its present state, the custom finite volumes code requires the geometry to be constructed out of rectangular shapes. Despite the rectangular boundaries, the propagation fronts in the callus assume curved shapes, which renders

this simplification acceptable as previously reported (Geris et al., 2006). However, upon the introduction of mechanical loading into the model, the jagged edge of the periosteal callus will cause singularities in the calculation of stresses and strains. Therefore, in future studies this aspect needs to be addressed. Other numerical tools (e.g. finite elements) might take away the restrictions on the shape of the domain but they would add other problems (e.g. the spatial integration of the taxis terms).

As discussed in Section 4.2, the boundary conditions for osteoblasts, endothelial cells and osteogenic growth factors were shown to have a significant influence on the spatial distribution of the various tissues in the callus region. These boundary conditions in fact arise from processes taking place in the cortex and the intact marrow. As neither cortex nor intact marrow were represented in the model, their influence on the regeneration process had to be captured by means of boundary conditions. A possible extension of the model could be to include the processes taking place in the cortex and the intact marrow. This would allow to remove the boundary conditions on the osteogenic growth factors, osteoblasts and endothelial cells. Meanwhile it might become possible to capture additional experimental observations e.g. the rounding of the cortical edges and the bony sealing of the marrow cavity in case of certain impaired healing situations (Harrison et al., 2003).

As indicated in Section 2.1, endothelial cell activation states were not explicitly addressed in this model. Endothelial cells can generally be divided according to two activation states, the active and the quiescent state. At the early stage of the angiogenic process, active endothelial cells are able to migrate and proliferate. Later on, they organise into blood vessel structures and become quiescent. When fractures occur, the quiescent endothelial cells can revert back to their active state as their organised matrix is disrupted (Lee and Gotlieb, 1999).

Similar to the lack of activation states, the differentiation from one cell type to another was not modelled to go through any transitory state. For example, osteogenic differentiation of mesenchymal stem cells passes through many intermediate states: osteoprogenitor, pre-osteoblast, transitory osteoblasts, secretory osteoblasts and the final state of maturation, the osteocyte (Bruder and Scaduto, 2005). All of these intermediate cell states have their specific functions. While in the model, osteoblasts are able to migrate, proliferate, produce matrix and express growth factors at the same time, in reality, all these functions are performed by different osteoblast intermediates. For chondrocytes, a distinction was made between the normal chondrocyte and its terminally differentiated state, the hypertrophic chondrocyte, by means of the cartilage matrix density. Activation states and differentiation intermediates could be included in the model by either extending the model framework to include new variables for every state (leading to a huge number of variables), or to include for each cell type a discrete value, indicating its activation or differentiation state.

Other important aspects of fracture healing which could be added to the model in the future include the role of oxygen gradients and oxygen concentration (Glowacki, 1998; Cramer et al., 2004), the role of matrix MMPs (Colnot et al., 2003; Ortega et al., 2004; Henle et al., 2005) and the interaction between the different growth factors (Peng et al., 2002).

4.5. Summary

The main goals for this study are the investigation of (1) different aspects of the fracture healing process and (2) possible causes of compromised fracture healing. An enhanced bioregulatory model, incorporating a number of the bone regeneration key features such as intramembranous and endochondral ossification, angiogenesis and cell migration has been established and its results have been successfully corroborated by comparison with experimental data of normal fracture healing. Furthermore, several cases of compromised fracture healing due to impaired angiogenesis have been simulated, predicting results similar to the experimental observations. Now that the model has been established, its possible therapeutic value can be tested. For example, simulating compromised healing situations, followed by injections of osteogenic and/or vascular growth factors at different points in time, can help to determine the optimal growth factor administration time and dosage needed to resume the normal healing process. Besides a possible therapeutic value, this model can also help to unravel the mechanisms of normal and compromised healing. By performing theoretical experiments, this model can help to identify interesting research questions.

Acknowledgements

Liesbet Geris is a post-doctoral research fellow of the Research Foundation Flanders (FWO-Vlaanderen). The authors wish to thank Prof. Goodship (RVC, London, UK) for providing the experimental data and his scientific advice.

Appendix

The following scalings were chosen for the non-dimensionalisation of the model variables:

$$\tilde{t}=\frac{t}{T},\quad \tilde{x_1}=\frac{x_1}{L},\quad \tilde{x_2}=\frac{x_2}{L},$$
$$\tilde{x_3}=\frac{x_3}{L},\quad \tilde{c_m}=\frac{c_m}{c_0},\quad \tilde{c_f}=\frac{c_f}{c_0},$$

$$\tilde{c_c}=\frac{c_c}{c_0},\quad \tilde{c_b}=\frac{c_b}{c_0},\quad \tilde{c_v}=\frac{c_v}{c_0},$$
$$\tilde{m_f}=\frac{m_f}{m_0},\quad \tilde{m_c}=\frac{m_c}{m_0},$$

$$\tilde{m}_b = \frac{m_b}{m_0}, \quad \tilde{m}_v = \frac{m_v}{m_0}, \quad \tilde{g}_c = \frac{g_c}{g_0},$$
$$\tilde{g}_b = \frac{g_b}{g_0}, \quad \tilde{g}_v = \frac{g_v}{g_0}.$$

Typical time and length scales for fracture healing in rodent studies are $T = 1$ day and $L = 3.5$ mm (Harrison et al., 2003). A representative concentration of the collagen content in the tissues under investigation is $m_0 = 0.1$ g/ml. Typical growth factor concentrations are in the order of magnitude of 10^{-9} M (mol/l) (Nogami and Oohira, 1984; Joyce et al., 1990). Taking into account the order of magnitude of the molecular weight of the growth factors (100 kDa = 100 kg/mol), this results in a non-dimensionalisation value of $g_0 = 100$ ng/ml. Based on geometrical constraints, Bailón-Plaza and van der Meulen (2001) derived a typical value for cell density at the beginning of the healing process: $c_0 = 10^6$ cells/ml.

The parameter values were derived from literature where possible and estimated when no relevant data were available:

- *Random motion and haptokinesis*: Microscopic studies of random movement of various cell types report diffusion constants D in the orders of magnitude of 10^{-8}–10^{-10} cm^2/s, depending on the cell type under investigation and the experimental conditions (Gruler and Bültmann, 1984; Friedl et al., 1998; Rupnick et al., 1988). For the haptokinetic coefficient (functional form (13)) used in this model, the maximum rate of cell motility occurs at a matrix density of $m = K_{hm}$ or $m = K_{hv}$ for mesenchymal stem cells and endothelial cells, respectively, yielding a value of $D_{hi} = 2K_{hi}D$ $(i = m, v)$. K_{hm} and K_{hv} were chosen positive and higher than the initial matrix density. The description of the random movement of fibroblasts was adopted directly from the model of Olsen et al. (1995), where a constant diffusion coefficient was used.
- *Chemotaxis*: Many experimental studies have investigated the chemotactic response of mesenchymal stem cells (Fiedler et al., 2004, 2005), fibroblasts (Seppä et al., 1982; Postlethwaite et al., 1987), osteoblasts (Lind et al., 1996; Mayr-Wohlfart et al., 2002) and endothelial cells (Stokes et al., 1990; Li et al., 2005) to various growth factors. Most of them report bell-shaped curves representing the migratory response to increasing growth factor concentrations. Maximal chemotactic response is reported for growth factor concentrations of 1–10 ng/ml. Based on the reported chemotactic coefficients for the different cell types, the values of the parameters involved in the description of chemotaxis were determined.
- *Haptotaxis*: In the absence of any available data for the haptotactic coefficients involved, the parameters were assigned values in the same order of magnitude as those of the chemotactic coefficients (Anderson and Chaplain, 1998; Bailón-Plaza and van der Meulen, 2001).
- *Proliferation*: Bailón-Plaza and van der Meulen (2001) derived for their model the values of the parameters of the proliferation function (16) for mesenchymal stem cells, chondrocytes and osteoblasts. Due to a lack of dedicated experimental data, these values were also adopted for the description of fibroblast and endothelial cell proliferation.
- *Differentiation*: Bailón-Plaza and van der Meulen (2001) examined, in the absence of quantified cell differentiation rates, different values for the parameters describing mesenchymal cell differentiation in a sensitivity analysis. The function representing the endochondral replacement (Bailón-Plaza and van der Meulen, 2001) was extended to encompass the influence of the angiogenic process. A parameter B_v was introduced, indicating that the endochondral replacement can only proceed when the vascularisation is increasing. One of the main regulators of the differentiation of mesenchymal stem cells towards fibroblasts seems to be mechanical load whereby a high mechanical load stimulates the formation of fibroblasts (Prendergast et al., 1997; Carter et al., 1998). However, this model does not explicitly treat the mechanical aspects of the regeneration process as discussed in Section 2. Therefore, as a first approximation, the differentiation rate of mesenchymal stem cells towards fibroblasts was taken to be a constant (F_4) (instead of a function of local mechanical stimuli). Furthermore, the value of the parameter F_4 is chosen small, implying that the majority of the fibroblasts present in the callus, have migrated from the surrounding tissues into the callus area.
- *Cell decay*: The rate of cell (osteoblast, fibroblast and endothelial) removal is not available from literature, and has been estimated by Bailón-Plaza and van der Meulen (2001) in a linear stability analysis for the case of the osteoblasts. A similar strategy was followed to determine the decay values for the other cell types described in this model.
- *Matrix synthesis and degradation*: Matrix synthesis rate was modelled to decrease proportionally with the increase of the corresponding matrix density. When the matrix density reaches its maximum value, the production will arrest. Initial production rates (P_{is}, $i = f, c, b, v$) were taken from Bailón-Plaza and van der Meulen (2001), based on the estimates calculated by Olsen et al. (1997).
- *Growth factor diffusion*: The diffusion coefficient of a chemical in an aqueous solution can be determined from its molecular weight, using a relation developed by Vander et al. (1998). Taking into account typical molecular weights of osteogenic and chondrogenic growth factors (Joyce et al., 1990), this leads to values for the diffusion coefficients in the order of magnitude of 10^{-8} cm^2/s. These values are corroborated by reported diffusion coefficients of various growth factors (Filion and Popel, 2004; Thorne et al., 2004). Reported diffusion coefficients for angiogenic growth factors

(Helm et al., 2005; Ambrosi et al., 2004) are in the order of magnitude of $10^{-7}\,cm^2/s$.

- *Growth factor production*: No experimental data are available on the production rates of growth factors. Therefore, a range of values for the magnitude of the production rate was explored numerically. The other parameter values (H_{gi}, $i = c, b, v$) were chosen in such a way that the saturation level for the production occurs around typical growth factor concentration levels.
- *Growth factor decay and consumption*: Typical values for the half-life of growth factors involved in fracture healing are around and below 30 min. (Coffey et al., 1990; Dasch et al., 1989; Edelman et al., 1993; Shima et al., 1995). A half-life of 10 min corresponds to a decay constant of $100\,day^{-1}$ (osteogenic and chondrogenic growth factors), a half-life of 30 min to a decay constant of $30\,day^{-1}$ (vascular growth factor). Consumption of the angiogenic growth factor by endothelial cells was modelled by a simple uptake function, of which the rate was determined numerically due to the lack of experimental data.

The model parameters were non-dimensionalised as follows (tildes referring to non-dimensionalised parameters):

$$\tilde{D}_{hm} = \frac{D_{hm}T}{L^2 m_0}, \quad \tilde{K}_{hm} = \frac{K_{hm}}{m_0}, \quad \tilde{C}_{kCTm} = \frac{C_{kCTm}T}{L^2},$$

$$\tilde{K}_{kCTm} = \frac{K_{kCTm}}{g_0}, \quad \tilde{C}_{kHTm} = \frac{C_{kHTm}T}{L^2 m_0}, \quad \tilde{K}_{kHTm} = \frac{K_{kHTm}}{m_0},$$

$$\tilde{A}_{m0} = \frac{A_{m0}T}{m_0}, \quad \tilde{K}_m = \frac{K_m}{m_0}, \quad \tilde{Y}_{11} = Y_{11}T,$$

$$\tilde{H}_{11} = \frac{H_{11}}{g_0}, \quad \tilde{Y}_{12} = Y_{12}, \quad \tilde{H}_{12} = \frac{H_{12}}{g_0},$$

$$\tilde{Y}_2 = Y_2 T, \quad \tilde{H}_2 = \frac{H_2}{g_0}, \quad \tilde{F}_4 = F_4 T,$$

$$\tilde{D}_f = \frac{D_f T}{L^2}, \quad \tilde{C}_{kf} = \frac{C_{kf}T}{L^2}, \quad \tilde{K}_{kf} = \frac{K_{kf}}{g_0},$$

$$\tilde{A}_{f0} = \frac{A_{f0}T}{m_0}, \quad \tilde{K}_f = \frac{K_f}{m_0}, \quad \tilde{Y}_5 = Y_5 T,$$

$$\tilde{H}_5 = \frac{H_5}{m_0}, \quad \tilde{B}_v = \frac{B_v}{m_0}, \quad \tilde{B}_{ec} = \frac{B_{ec}}{m_0},$$

$$\tilde{Y}_3 = Y_3 T, \quad \tilde{H}_3 = \frac{H_3}{g_0}, \quad \tilde{d}_f = d_f,$$

$$\tilde{A}_{c0} = \frac{A_{c0}T}{m_0}, \quad \tilde{K}_c = \frac{K_c}{m_0}, \quad \tilde{C}_{kb} = \frac{C_{kb}T}{L^2},$$

$$\tilde{K}_{kb} = \frac{K_{kb}}{g_0}, \quad \tilde{A}_{b0} = \frac{A_{b0}T}{m_0}, \quad \tilde{K}_b = \frac{K_b}{m_0},$$

$$\tilde{d}_b = d_b T, \quad \tilde{D}_{hv} = \frac{D_{hv}T}{L^2 m_0}, \quad \tilde{K}_{hv} = \frac{K_{hv}}{m_0},$$

$$\tilde{C}_{kCTv} = \frac{C_{kCTv}T}{L^2}, \quad \tilde{K}_{kCTv} = \frac{K_{kCTv}}{g_0}, \quad \tilde{C}_{v_{HT}} = \frac{C_{v_{HT}}Tm_0}{L^2},$$

$$\tilde{A}_{v0} = \frac{A_{v0}T}{m_0}, \quad \tilde{K}_v = \frac{K_v}{m_0}, \quad \tilde{d}_v = d_v T,$$

$$\tilde{P}_{fs} = \frac{P_{fs}Tc_0}{m_0}, \quad \tilde{Q}_f = Q_f m_0 c_0 T, \quad \tilde{P}_{cs} = \frac{P_{cs}Tc_0}{m_0},$$

$$\tilde{Q}_c = Q_c c_0 T, \quad \tilde{P}_{bs} = \frac{P_{bs}Tc_0}{m_0}, \quad \tilde{P}_{vs} = \frac{P_{vs}Tc_0}{m_0},$$

$$\tilde{D}_{gc} = \frac{D_{gc}T}{L^2}, \quad \tilde{G}_{gc} = \frac{G_{gc}Tc_0}{g_0 m_0^2}, \quad \tilde{H}_{gc} = \frac{H_{gc}}{g_0},$$

$$\tilde{K}_{gc} = \frac{K_{gc}}{m_0}, \quad \tilde{d}_{gc} = d_{gc}T, \quad \tilde{D}_{gb} = \frac{D_{gb}T}{L^2},$$

$$\tilde{G}_{gb} = \frac{G_{gb}Tc_0}{g_0}, \quad \tilde{H}_{gb} = \frac{H_{gb}}{g_0}, \quad \tilde{d}_{gb} = d_{gb}T.$$

This resulted in the following set of non-dimensional parameter values: $\tilde{D}_{hm} = 0.014$, $\tilde{K}_{hm} = 0.25$, $\tilde{C}_{kCTm} = 0.04$, $\tilde{K}_{kCTm} = 0.1$, $\tilde{C}_{kHTm} = 0.0034$, $\tilde{K}_{kHTm} = 0.5$, $\tilde{A}_{m0} = 1.01$, $\tilde{K}_m = 0.1$, $\tilde{\alpha}_m = 1$, $\tilde{Y}_{11} = 10$, $\tilde{H}_{11} = 0.1$, $\tilde{Y}_{12} = 2$, $\tilde{H}_{12} = 0.1$, $\tilde{Y}_2 = 50$, $\tilde{H}_2 = 0.1$, $\tilde{F}_4 = 0.001$, $\tilde{D}_f = 0.02$, $\tilde{C}_{kf} = 0.4$, $\tilde{K}_{kf} = 0.1$, $\tilde{A}_{f0} = 0.202$, $\tilde{K}_f = 0.1$, $\tilde{\alpha}_f = 1$, $\tilde{Y}_5 = 50$, $\tilde{H}_5 = 0.1$, $\tilde{B}_v = 0.3 \times 10^{-7}$, $\tilde{B}_{ec} = 1.5$, $\tilde{Y}_3 = 1000$, $\tilde{H}_3 = 0.1$, $\tilde{d}_f = 0.1$, $\tilde{A}_{c0} = 0.101$, $\tilde{K}_c = 0.1$, $\tilde{\alpha}_c = 1$, $\tilde{C}_{kb} = 1.4 \times 10^{-8}$, $\tilde{K}_{kb} = 0.01$ $\tilde{A}_{b0} = 0.202$, $\tilde{K}_b = 0.1$, $\tilde{\alpha}_b = 1$, $\tilde{d}_b = 0.1$, $\tilde{D}_{hv} = 0.00007$, $\tilde{K}_{hv} = 1$, $\tilde{C}_{kCTv} = 0.0306$, $\tilde{K}_{kCTv} = 0.025$, $\tilde{C}_{v_{HT}} = 10^4$, $\tilde{A}_{v0} = 0.202$, $\tilde{K}_v = 0.1$, $\tilde{\alpha}_v = 1$, $\tilde{d}_v = 0.1$, $\tilde{P}_{fs} = 0.2$, $\tilde{\kappa}_f = 1$, $\tilde{Q}_f = 1.5$,$\tilde{P}_{cs} = 0.2$, $\tilde{\kappa}_c = 1$, $\tilde{Q}_c = 1.5$, $\tilde{P}_{bs} = 2$, $\tilde{\kappa}_b = 1$, $\tilde{P}_{vs} = 2 \times 10^{-6}$, $\tilde{\kappa}_v = 10^6$, $\tilde{D}_{gc} = 0.005$, $\tilde{G}_{gc} = 50$, $\tilde{H}_{gc} = 1$, $\tilde{K}_{gc} = 0.1$, $\tilde{d}_{gc} = 100$, $\tilde{D}_{gb} = 0.005$, $\tilde{G}_{gb} = 500$, $\tilde{H}_{gb} = 1$, $\tilde{d}_{gb} = 100$, $\tilde{D}_{gv} = 0.5$, $\tilde{G}_{gvb} = 10^{-11}$, $\tilde{H}_{gv} = 1$, $\tilde{K}_{gv} = 10^{-6}$, $\tilde{G}_{gvc} = 10^{-3}$, $\tilde{d}_{gv} = 30$, $\tilde{d}_{gvc} = 200\,000$.

References

Ahrens, M., Ankenbauer, T., Schroder, D., Hollnagel, A., Mayer, H., Gross, G., 1993. Expression of human bone morphogenetic proteins-2 or -4 in murine mesenchymal progenitor C3H10T1/2 cells induces differentiation into distinct mesenchymal cell lineages. DNA Cell Biol. 12 (10), 871–880.

Ambrosi, D., Gamba, A., Serini, G., 2004. Cell directional and chemotaxis in vascular morphogenesis. Bull. Math. Biol. 66, 1851–1873.

Amir, L.R., Becking, A.G., Jovanovic, A., Perdijk, F.B., Everts, V., Bronckers, A.L., 2006. Formation of new bone during vertical distraction osteogenesis of the human mandible is related to the presence of blood vessels. Clin. Oral Implants Res. 17 (4), 410–416.

Anderson, A.R.A., Chaplain, M.A.J., 1998. Continuous and discrete mathematical models of tumor-induced angiogenesis. Bull. Math. Biol. 60, 857–900.

Bailón-Plaza, A., van der Meulen, M.C.H., 2001. A mathematical framework to study the effects of growth factor influences on fracture healing. J. Theor. Biol. 212, 191–209.

Bailón-Plaza, A., van der Meulen, M.C.H., 2003. Beneficial effects of moderate, early loading and adverse effects of delayed or excessive loading on bone healing. J. Biomech. 36, 1069–1077.

Bancroft, G.N., Sikavitsas, V.I., van den Dolder, J., Sheffield, T.L., Ambrose, C.G., Jansen, J.A., Mikos, A.G., 2002. Fluid flow increases mineralized matrix deposition in 3D perfusion culture of marrow stromal osteoblasts in a dose-dependent manner. Proc. Natl Acad. Sci. 99 (20), 12600–12605.

Barnes, G.L., Kostenuik, P.J., Gerstenfeld, L.C., Einhorn, T.A., 1999. Growth factor regulation of fracture repair. J. Bone Miner. Res. 14 (11), 1805–1815.

Bland, Y.S., Critchlow, M.A., Ashhurst, D.E., 1999. The expression of the fibrillar collagen genes during fracture healing: heterogeneity of the matrices and differentiation of the osteoprogenitor cells. Histochem. J. 31, 797–809.

Bolander, M.E., 1992. Regulation of fracture repair by growth factors. Proc. Soc. Exp. Biol. Med. 200, 165–170.

Bruder, S.P., Scaduto, T., 2005. Cell-based strategies for bone regeneration: from developmental biology to clinical therapy. In: Lieberman, J.R., Friedlaender, G.E. (Eds.), Bone Regeneration and Repair: Biology and Clinical Applications. Humana Press Inc, Otowa, NJ, pp. 67–92.

Carano, R.A.D., Filvaroff, E.H., 2003. Angiogenesis and bone repair. Drug Discovery Today 8 (21), 980–989.

Carter, D.R., Beaupré, G.S., Giori, N.J., Helms, J.A., 1998. Mechanobiology of skeletal regeneration. Clin. Orthop. Relat. Res. 355S, S41–S55.

Chai, B., Tang, X., Li, H., 1999. Osteogenic role played by fibroblasts in secondary healing of fracture. Chin. J. Traumatol. 2, 53–56.

Claes, L.E., Heigele, C.A., Neidlinger-Wilke, C., Kaspar, D., Seidl, W., Margevicius, K.J., Augat, P., 1998. Effects of mechanical factors on the fracture healing process. Clin. Orthop. Relat. Res. 355S, S132–S147.

Coffey, R.J., Russell, W.E., Barnard, J.A., 1990. Pharmacokinetics of TGF beta with emphasis on effects in liver and gut. Ann. N.Y. Acad. Sci. 593, 285–291.

Colnot, C., Thompson, Z., Miclau, T., Werb, Z., Helms, J.A., 2003. Altered fracture repair in the absence of MMP9. Development 130, 4123–4133.

Cramer, T., Schipani, E., Johnson, R.S., Swoboda, B., Pfander, D., 2004. Expression of VEGF isoforms by epiphyseal chondrocytes during low-oxygen tension is HIF-1alfa dependent. Osteoarthr. Cart. 12, 433–439.

Darling, E.M., Athanasiou, K.A., 2003. Articular cartilage bioreactors and bioprocesses. Tissue Eng. 1, 9–26.

Dasch, J.R., Pace, D.R., Waegell, W., Inenaga, D., Ellingsworth, L., 1989. Monoclonal antibodies recognizing transforming growth factor-beta. Bioactivity neutralization and transforming growth factor beta 2 affinity purification. J. Immunol. 142, 1536–1541.

Deckers, M.M., Karperien, M., van der Bent, C., Yamashita, T., Papapoulos, S.E., Lowik, C.W., 2000. Expression of vascular endothelial growth factors and their receptors during osteoblast differentiation. Endocrinology 141 (5), 1667–1674.

Deckers, M.M., van Beek, E.R., van der Pluijm, G., Wetterwald, A., van der Wee-Pals, L.J.A., Cecchini, M.G., Papapoulos, S.E., Lowik, C.W., 2002. Dissociation of angiogenesis and osteoclastogenesis during endochondral bone formation in neonatal mice. J. Bone Miner. Res. 17, 998–1007.

Dickinson, R.B., Tranquillo, R.T., 1993. A stochastic model for adhesion-mediated cell random motility and haptokinesis. J. Math. Biol. 31, 563–600.

Dimitriou, R., Tsiridis, E., Giannoudis, P.V., 2005. Current concepts of molecular aspects of bone healing. Injury 36 (12), 1392–1404.

Edelman, E.R., Nugent, M.A., Karnovsky, M.J., 1993. Perivascular and intravenous administration of basic fibroblast growth factor: vascular and solid organ deposition. Proc. Natl Acad. Sci. USA 90, 1513–1517.

Ehrlich, P.J., Lanyon, L.E., 2002. Mechanical strain and bone cell function: a review. Osteoporos. Int. 13, 688–700.

Einhorn, T.A., 1995. Enhancement of fracture healing. J. Bone J. Surg. Am. 77, 940–956.

Einhorn, T.A., 1998. The cell and molecular biology of fracture healing. Clin. Orthop. Relat. Res. 355S, S7–S21.

Enomoto-Iwamoto, M., Iwamoto, M., Mukudai, Y., Kawakami, Y., Nohno, T., Higuchi, Y., Takemoto, S., Ohuchi, H., Noji, S., Kurisu, K., 1998. Bone morphogenetic protein signaling is required for maintenance of differentiated phenotype, control of proliferation, and hypertrophy in chondrocytes. J. Cell Biol. 140, 409–418.

Fang, T.D., Salim, A., Xia, W., Nacamuli, R.P., Guccione, S., Song, H.M., Carano, R.A., Filvaroff, E.H., Bednarski, M.D., Giaccia, A.J., Longaker, M.T., 2005. Angiogenesis is required for successful bone induction during distraction osteogenesis. J. Bone Miner. Res. 20 (7), 1114–1124.

Fiedler, J., Etzel, N., Brenner, R., 2004. To go or not to go: migration of human mesenchymal progenitor cells stimulated by isoforms of PDGF. J. Cell. Biochem. 93, 990–998.

Fiedler, J., Leucht, F., Waltenberger, J., Dehio, C., Brenner, R.E., 2005. VEGF-A and PlGF-1 stimulate chemotactic migration of human mesenchymal progenitor cells. Biochem. Biophys. Res. Commun. 334, 561–568.

Filion, R.J., Popel, A.S., 2004. A reaction–diffusion model of basic fibroblast growth factor interactions with cell surface receptors. Ann. Biomed. Eng. 32, 645–663.

Friedl, P., Zänker, K.S., Bröcker, E.B., 1998. Cell migration strategies in 3-d extracellular matrix: differences in morphology, cell matrix interactions, and integrin function. Microsc. Res. Tech. 43, 369–378.

Gerber, H.-P., Vu, T.H., Ryan, A.M., Kowalski, J., Werb, Z., Ferrara, N., 1999. VEGF couples hypertrophic cartilage remodeling, ossification and angiogenesis during endochondral bone formation. Nat. Med. 5, 623–628.

Geris, L., Van Oosterwyck, H., Vander Sloten, J., Duyck, J., Naert, I., 2003. Assessment of mechanobiological models for the numerical simulation of tissue differentiation around immediately loaded implants. Comp. Methods Biomech. Biomed. Eng. 6, 277–288.

Geris, L., Andreykiv, A., Van Oosterwyck, H., Vander Sloten, J., van Keulen, F., Duyckc, J., Naert, I., 2004. Numerical simulation of tissue differentiation around loaded titanium implants in a bone chamber. J. Biomech. 37, 763–769.

Geris, L., Gerisch, A., Maes, C., Carmeliet, G., Weiner, R., Vander Sloten, J., Van Oosterwyck, H., 2006. Mathematical modeling of fracture healing in mice: comparison between experimental data and numerical simulation results. Med. Biol. Eng. Comp. 44 (4), 280–289.

Geris, L., Vandamme, K., Naert, I., Vander Sloten, J., Duyck, J., Van Oosterwyck, H., 2007. Application of mechanoregulatory models to simulate peri-implant tissue formation in an in vivo bone chamber. J. Biomech. doi:10.1016/j.jbiomech.2007.07.008.

Gerisch, A., 2001. Numerical methods for the simulation of taxis–diffusion–reaction systems. Ph.D. Thesis, Martin-Luther-Universität Halle-Wittenberg, Germany.

Gerisch, A., Chaplain, M.A.J., 2005. Robust numerical methods for taxis–diffusion–reaction systems: applications to biomedical problems. Math. Comput. Model. 43, 49–75.

Gerisch, A., Geris, L., 2007. A finite volume spatial discretisation for taxis–diffusion–reaction systems with axi-symmetry: application to fracture healing. In: Deutsch, A., Brusch, L., Byrne, H., de Vries, G., Herzel, H.P. (Eds.), Advances in Mathematical Modeling of Biological Systems, vol. I. Birkhäuser, Boston, pp. 299–311.

Gerstenfeld, L.C., Cullinane, D.M., Barnes, G.L., Graves, D.T., Einhorn, T.A., 2003a. Fracture healing as a post-natal developmental process: molecular, spatial, and temporal aspects of its regulation. J. Cell. Biochem. 88, 873–884.

Glowacki, J., 1998. Angiogenesis in fracture repair. Clin. Orthop. Rel. Res. 355S, S82–S89.

Gómez-Benito, M.J., García-Aznar, J.M., Kuiper, J.H., Doblaré, M., 2005. Influence of fracture gap size on the pattern of long bone healing: a computational study. J. Theor. Biol. 235, 105–119.

Gruler, H., Bültmann, B.D., 1984. Analysis of cell movement. Blood cells 10, 61–77.

Guenther, H.L., Fleisch, H., Sorgente, N., 1986. Endothelial cells in culture secrete a potent bone cell active mitogen. Endocrinology 119, 193–201.

Hadjiargyrou, M., Lombardo, F., Zhao, S., Ahrens, W., Joo, J., Ahn, H., Jurman, M., White, D.W., Rubin, C.T., 2002. Transcriptional profiling of bone regeneration. J. Biol. Chem. 277 (33), 30177–30182.

Harrison, L.J., Cunningham, J.L., Strömberg, L., Goodship, A.E., 2003. Controlled induction of a pseudarthrosis: a study using a rodent model. J. Orthop. Trauma 17, 11–21.

Hee, C.K., Jonikas, M.A., Nicoll, S.B., 2006. Influence of three-dimensional scaffold on the expression of osteogenic differentiation markers by human dermal fibroblasts. Biomaterials 27 (6), 875–884.

Helm, C.E., Fleury, M.E., Zisch, A.H., Boschetti, F., Swartz, M.A., 2005. Synergy between interstitial flow and VEGF directs capillary morphogenesis in vitro through a gradient amplification mechanism. Proc. Natl Acad. Sci. USA 102, 15779–15784.

Henle, P., Zimmermann, G., Weiss, S., 2005. Matrix metalloproteinases and failed fracture healing. Bone 37, 791–798.

Hundsdorfer, W., Verwer, J.G., 2003. Numerical solution of time-dependent advection–diffusion–reaction equations. Springer Series in Computational Mathematics, vol. 33. Springer, Berlin.

Isaksson, H., Comas, O., van Donkelaar, C., Mediavilla, J., Wilson, W., Huiskes, R., Ito, K., 2006. Bone regeneration during distraction osteogenesis: mechano-regulation by shear strain and fluid velocity. J. Biomech, available online.

Jagodzinski, M., Drescher, M., Zeichen, J., Hankemeier, S., Krettek, C., Bosch, U., van Griensven, M., 2004. Effects of cyclic longitudinal mechanical strain and dexamethasone on osteogenic differentiation of human bone marrow stromal cells. Eur. Cell Mater. 7, 35–41.

Joyce, M.E., Terek, R.M., Jingushi, S., Bolander, M.E., 1990. Role of transforming growth factor-b in fracture repair. Ann. N. Y. Acad. Sci. 593, 107–123.

Kaspar, D., Seidl, W., Neidlinger-Wilke, C., Ignatius, A., Claes, L., 2000. Dynamic cell stretching increases human osteoblast proliferation and CICP synthesis but decreases osteocalcin synthesis and alkaline phosphatase activity. J. Biomech. 33, 45–51.

Kasperk, C.H., Börcsök, I., Schairer, H.U., Schneider, U., Nawroth, P.P., Niethard, F.U., Ziegler, R., 1997. Endothelin-1 is a potent regulator of human bone cell metabolism *in vitro*. Calcif. Tissue Int. 60, 368–374.

Knippenberg, M., Helder, M.N., Doulabi, B.Z., Semeins, C.M., Wuisman, P.I., Klein-Nulend, J., 2005. Adipose tissue-derived mesenchymal stem cells acquire bone cell-like responsiveness to fluid shear stress on osteogenic stimulation. Tissue Eng. 11 (11–12), 1780–1788.

Kreke, M.R., Huckle, W.R., Goldstein, A.S., 2005. Fluid flow stimulates expression of osteopontin and bone sialoprotein by bone marrow stromal cells in a temporally dependent manner. Bone 36 (6), 1047–1055.

Kuntz, R.M., Saltzman, W.M., 1997. Neutrophil motility in extra-cellular matrix gels: mesh size and adhesion affect speed of migration. Biophys. J. 72 (3), 1472–1480.

Lacroix, D., Prendergast, P.J., 2002. A mechano-regulation model for tissue differentiation during fracture healing: analysis of gap size and loading. J. Biomech. 35, 1163–1171.

Laplantine, E., Rossi, F., Sahni, M., Basilico, C., Cobrinik, D., 2002. FGF signaling targets the pRb-related p107 and p130 proteins to induce chondrocyte growth arrest. J. Cell Biol. 158, 741–750.

Lee, T.-Y.J., Gotlieb, A.I., 1999. Early stages of endothelial wound repair: conversion of quiescent to migrating endothelial cells involves tyrosine phosphorylation and actin microfilament reorganization. Cell Tissue Res. 297, 435–450.

Li, Y.J., Batra, N.N., You, L., Meier, S.C., Coe, I.A., Yellowley, C.E., Jacobs, C.R., 2004. Oscillatory fluid flow affects human marrow stromal cell proliferation and differentiation. J. Orthop. Res. 22, 1283–1289.

Li, G., Cui, Y., McIlmurray, L., Allen, W.A., Wang, H., 2005. rhBMP-2, rhVEGF165, rhPTN and thrombin-related peptide, TP508 induce chemotaxis of human osteoblasts and microvascular endothelial cells. J. Orthop. Res. 23, 680–685.

Lienau, J., Schell, H., Duda, G.N., Seebeck, P., Muchow, S., Bail, H.J., 2005. Initial vascularization and tissue differentiation are influenced by fixation stability. J Orthop. Res. 23 (3), 639–645.

Lin, W.L., McCulloch, C.A., Cho, M.I., 1994. Differentiation of periodontal ligament fibroblasts into osteoblasts during socket healing after tooth extraction in the rat. Anat. Rec. 240 (4), 492–506.

Lind, M., Eriksen, E.F., Bünger, C., 1996. Bone morphogenetic protein-2 but not bone morphogenetic protein-4 and -6 stimulates chemotactic migration of human osteoblasts, human marrow osteoblasts, and U2-OS cells. Bone 18, 53–57.

Lu, C., Miclau, T., Hu, D., Marcucio, R.S., 2007. Ischemia leads to delayed union during fracture healing: a mouse model. J. Orthop. Res. 25 (1), 51–61.

Lutolf, M.P., Lauer-Fields, J.L., Schmoekel, H.G., Metters, A.T., Weber, F.E., Fields, G.B., Hubbell, J.A., 2003. Synthetic matrix metalloproteinase-sensitive hydrogels for the conduction of tissue regeneration: engineering cell-invasion characteristics. Proc. Natl Acad. Sci. 100 (9), 5413–5418.

Maes, C., 2004. Angiogenesis and bone: the role of the vascular endothelial growth factor family in bone development and repair. Ph.D. Thesis (Acta Biomedica Lovaniensia 310), Leuven University Press, Leuven, Belgium.

Maes, C., Carmeliet, P., Moermans, K., Stockmans, I., Smets, N., Collen, D., Bouillon, R., Carmeliet, G., 2002. Impaired angiogenesis and endochondral bone formation in mice lacking the vascular endothelial growth factor isoforms VEGF164 and VEGF188. Mech. Dev. 111, 61–73.

Maes, C., Coenegrachts, L., Stockmans, I., Daci, E., Luttun, A., Petryk, A., Gopalakrishnan, R., Moermans, K., Smets, N., Verfaillie, C.M., Carmeliet, P., Bouillon, R., Carmeliet, G., 2006. Placental growth factor mediates mesenchymal cell development, cartilage turnover, and bone remodeling during fracture repair. J. Clin. Invest. 116, 1230–1242.

Maheswari, G., Wells, A., Griffith, L.G., Lauffenburger, D.A., 1999. Biophysical integration of effects of epidermal growth factor and fibronectin on fibroblast migration. Biophys. J. 76, 2814–2823.

Malizos, K.N., Papatheodorou, L.K., 2005. The healing potential of the periosteum, molecular aspects. Injury 36S, S13–S19.

Mayer, H., Bertram, H., Lindenmaier, W., Korff, T., Weber, H., Weich, H., 2005. Vascular endothelial growth factor (VEGF-A) expression in human mesenchymal stem cells: autocrine and paracrine role on osteoblastic and endothelial differentiation. J. Cell. Biochem. 95, 827–839.

Mayr-Wohlfart, U., Waltenberger, J., Hausser, H., Kessler, S., Günther, K.-P., Dehio, C., Puhl, W., Brenner, R.E., 2002. Vascular endothelial growth factor stimulates chemotactic migration of primary human osteoblasts. Bone 30, 472–477.

Metheny-Barlow, L.J., Tian, S., Hayes, A.J., Li, L.Y., 2004. Direct chemotactic action of angiopoietin-1 on mesenchymal cells in the presence of VEGF. Microvasc. Res. 68, 221–230.

Michaeli, Y., Shamir, D., Weinreb, M., Steigman, S., 1994. Effect of loading on the migration of periodontal fibroblasts in the rat incisor. J Periodontal Res. 29 (1), 25–34.

Midy, V., Plouet, J., 1994. Vasculotropin/vascular endothelial growth factor induces differentiation in cultured osteoblasts. Biochem. Biophys. Res. Commun. 199, 380–386.

Nagy, J.A., Senger, D.R., 2006. VEGF-A, cytoskeletal dynamics, and the pathological vascular phenotype. Exp. Cell Res. 312, 538–548.

Nogami, H., Oohira, A., 1984. Postnatal new bone formation. Clin. Orthop. Relat. Res. 184, 106–113.

Olsen, L., Sherratt, J., Maini, P., 1995. A mechanochemical model for adult dermal wound contraction and the permanence of the contracted tissue displacement profile. J. Theor. Biol. 177, 113–128.

Olsen, L., Sherratt, J., Maini, P., Arnold, F., 1997. A mathematical model for the capillary endothelial cell-extracellular matrix interactions in

wound-healing angiogenesis. IMA J. Math. Appl. Med. Biol. 14, 261–281.

Ortega, N., Behonick, D.J., Werb, Z., 2004. Matrix remodeling during endochondral ossification. Trends Cell Biol. 14 (2), 86–93.

Peng, H., Wright, V., Usas, A., Gearhart, B., Shen, H.C., Cummins, J., Huard, J., 2002. Synergistic enhancement of bone formation and healing by stem cell-expressed VEGF and bone morphogenetic protein-4. J. Clin. Invest. 110 (6), 751–759.

Postlethwaite, A.E., Keski-Oja, J., Moses, H.L., Kang, A.H., 1987. Simulation of the chemotactic migration of human fibroblasts by transforming growth factor β. J. Exp. Med. 165, 251–256.

Pountos, I., Giannoudis, P.V., 2005. Biology of mesenchymal stem cells. Injury 36S, S8–S12.

Prendergast, P.J., Huiskes, R., Søballe, K., 1997. Biophysical stimuli on cells during tissue differentiation at implant interfaces. J. Biomech. 30, 539–548.

Pufe, T., Kurz, B., Petersen, W., Varoga, D., Mentlein, R., Kulow, S., Lemke, A., Tillmann, B., 2005. The influence of biomechanical parameters on the expression of VEGF and endostatin in the bone and joint system. Ann. Anat. 187 (5–6), 461–472.

Rickard, D.J., Sullivan, T.A., Shenker, B.J., Leboy, P.S., Kazhdan, I., 1994. Induction of rapid osteoblast differentiation in rat bone marrow stromal cell cultures by dexamethasone and BMP-2. Dev. Biol. 161 (1), 218–228.

Rossi, F., MacLean, H.E., Yuan, W., Francis, R.O., Semenova, E., Lin, C.S., Kronenberg, H.M., Cobrinik, D., 2002. p107 and p130 coordinately regulate proliferation, Cbfa1 expression, and hypertrophic differentiation during endochondral bone development. Dev. Biol. 247, 271–285.

Rupnick, M.A., Stokes, C.L., Williams, S.K., Lauffenburger, D.A., 1988. Quantitative analysis of human microvessel endothelial cells using a linear under-agarose assay. Lab. Invest. 59, 363–372.

Sakai, K., Mohtai, M., Iwamoto, Y., 1998. Fluid shear stress increases transforming growth factor beta 1 expression in human osteoblast-like cells: modulation by cation channel blockades. Calcif. Tissue Int. 63 (6), 515–520.

Sato, Y., Rifkin, D.B., 1988. Autocrine activities of basic FGF: regulation of cell movement, plasminogen activator synthesis and DNA synthesis. J. Cell. Biol. 107, 1199–1205.

Seppä, H., Grotendorst, G., Seppä, S., Schiffmann, E., Martin, G.R., 1982. Platelet-derived growth factor is chemotactic for fibroblasts. J. Cell Biol. 92, 584–588.

Shefelbine, S.J., Augat, P., Claes, L., Simon, U., 2005. Trabecular bone fracture healing simulation with finite element analysis and fuzzy logic. J. Biomech. 38 (12), 2440–2450.

Sherratt, J., 1994. Chemotaxis and chemokinesis in eukaryotic cells: the Keller–Segel equations as an approximation to a detailed model. Bull. Math. Biol. 56, 129–146.

Shima, D.T., Deutsch, U., D'Amore, P.A., 1995. Hypoxic induction of vascular endothelial growth factor (VEGF) in human epithelial cells is mediated by increases in mRNA stability. FEBS Lett. 370, 203–208.

Stokes, C.L., Rupnick, M.A., Williams, S.K., Lauffenburger, D.A., 1990. Chemotaxis of human microvessel endothelial cells in response to acidic fibroblast growth factor. Lab. Invest. 63, 657–668.

Street, J., Bao, M., deGuzman, L., Bunting, S., Peale Jr., F.V., Ferrara, N., Steinmetz, H., Hoeffel, J., Cleland, J.L., Daugherty, A., van Bruggen, N., Redmond, H.P., Carano, R.A.D., Filvaroff, E.H., 2002. Vascular endothelial growth factor stimulates bone repair by promoting angiogenesis and bone turnover. Proc. Natl Acad. Sci. USA 99 (15), 9656–9661.

Taguchi, K., Ogawa, R., Migita, M., Hanawa, H., Ito, H., Orimo, H., 2005. The role of bone marrow-derived cells in bone fracture repair in a green fluorescent protein chimeric mouse model. Biochem. Biophys. Res. Commun. 331, 31–36.

Terranova, V.P., Diflorio, R., Lyall, R.M., Hic, S., Friesel, R., Maciag, T., 1985. Human endothelial cells are chemotactic to endothelial cell growth factor and heparin. J. Cell Biol. 101, 2330–2334.

Thies, R.S., Bauduy, M., Ashton, B.A., Kurtzberg, L., Wozney, J.M., Rosen, V., 1992. Recombinant human bone morphogenetic protein-2 induces osteoblastic differentiation in W-20-17 stromal cells. Endocrinology 130 (3), 1318–1324.

Thorne, R.G., Hrabetova, S., Nicholson, C., 2004. Diffusion of epidermal growth factor in rat brain extracellular space measured by integrative optical imaging. J. Neurophysiol. 92, 3471–3481.

Vander, A., Sherman, J., Luciano, D., 1998. Human Physiology: The Mechanisms of Body Function. WCB McGraw-Hill, Boston, MA.

Villenueva, J.E., Nimni, M.E., 1997. Promotion of calvarial cell osteogenesis by endothelial cells. J. Bone Miner. Res. 5, 733–739.

Weinberg, C.B., Bell, E., 1985. Regulation of proliferation of bovine aortic endothelial cells, smooth muscle cells and adventitial fibroblasts in collagen lattices. J. Cell. Physiol. 122, 410–414.

Weiner, R., Schmitt, B.A., Podhaisky, H., 1997. ROWMAP—a ROW-code with Krylov techniques for large stiff ODEs. Appl. Numer. Math. 25, 303–319.

Yoshizato, K., Taira, T., Yamamoto, N., 1985. Growth inhibition of human fibroblasts by reconstituted collagen fibrils. Biomed. Res. 6, 61–71.

Zaman, M.H., Trapani, L.M., Sieminski, A.L., MacKellar, D., Gong, H., Kamm, R.D., Wells, A., Lauffenburger, D.A., Matsudaira, P., 2006. Migration of tumor cells in 3D matrices is governed by matrix stiffness along with cell-matrix adhesion and proteolysis. Proc. Natl Acad. Sci. 103 (29), 10889–10894.

Zhang, X., Sui, S., Bao, K., Zeng, B., 2001. Osteoporosis influence the fracture healing in ovariectomized rat: ultrastructure study. Chin. Med. J. 114, 15–21.